Efficiency functionals for the Lévy flight foraging hypothesis

Serena Dipierro, Giovanni Giacomin and Enrico Valdinoci *

May 19, 2021

Abstract

We consider a forager diffusing via a fractional heat equation and we introduce several efficiency functionals whose optimality is discussed in relation to the Lévy exponent of the evolution equation.

Several biological scenarios, such as a target close to the forager, a sparse environment, a target located away from the forager and two targets are specifically taken into account.

The optimal strategies of each of these configurations are here analyzed explicitly also with the aid of some special functions of classical flavor and the results are confronted with the existing paradigms of the Lévy foraging hypothesis.

Interestingly, one discovers bifurcation phenomena in which a sudden switch occurs between an optimal (but somehow unreliable) Lévy foraging pattern of inverse square law type and a less ideal (but somehow more secure) classical Brownian motion strategy.

Additionally, optimal foraging strategies can be detected in the vicinity of the Brownian one even in cases in which the Brownian one is pessimizing an efficiency functional.

1 Introduction

Foraging theory (see e.g. [47]) is a fascinating, important and cross-disciplinary topic of investigation that gathers together researchers from different areas (such as biologists, ethologists, physicists, statisticians, computer scientists, mathematicians, etc.). It is commonly accepted that the broad variety of environmental and biological situations in nature and the Darwinistic evolution through natural selection have led over time to highly efficient foraging strategies see e.g. [6] (it is however under an intense debate whether Lévy type patterns in animal searches are an evolutionary stable and well consolidated outcome [24] or they are produced by innate composite correlated random walks [7, 38]; under investigation is also the role of particular distribution of resources for the emergence of foraging patterns, see e.g. [9]; it is also debatable that natural selection alone can always optimize a specific parameter in complex environments, see e.g. [21, 32]).

In general, the precise determination of optimal foraging strategies depends in a very complex way on a large number of parameters (such as the density and mobility of the preys and of the searchers and the mutable environmental conditions); furthermore, the collection and analysis of empirical data are typically challenging tasks, also open to controversial interpretations due to the use of different mathematical models or even due to spurious information (see e.g. [16]).

*Department of Mathematics and Statistics, University of Western Australia, 35 Stirling Highway, WA6009 Crawley, Australia.
serena.dipierro@uwa.edu.au, giovanni.giacomin.1@studenti.unipd.it, enrico.valdinoci@uwa.edu.au

A rather consolidated attempt to understand and classify different foraging strategies according to the evolution of the distribution of the searchers lies in the so-called Lévy flight foraging hypothesis. Namely, rather than diffusing in analogy to the classical Brownian motion, empirical evidence has often backed the hypothesis that animals move according to a scale-free fractal-like pattern similar to the one produced by long-jump random walks of Lévy type, possibly to avoid being trapped in a search of food confined in a narrow region beyond sensory range and to reduce the chances of intensively revisiting immediate surrounding areas in environments of scarce resources (see e.g. [46, 23, 24, 25] for empirical evidence for such biological Lévy flights). Phenomena related to Lévy flights are attracting increasing interest and they seem to possess some kind of universality, occurring also in situations different from animal foraging and including, among the others, human settlements and travels, see [8, 10, 11, 20, 36, 39] and also [17] for related virtual reconstructions. Lévy patterns also emerge in dynamical models as a non-Gaussian transport related to chaos, see e.g. [3, 45].

Several studies have exploited tools from mathematical analysis and statistical mechanics to validate the hypothesis that Lévy flights confer a significant advantage for foragers, see [51, 5, 50, 37]. Typically, to confirm the Lévy flights optimality, structural assumptions on the environment, on the searcher and on the target are taken, such as: the foraging should be of non-destructive type (that is, once a target has been foraged, it has to reappear infinitely fast); after foraging, the seeker starts a new flight "infinitely close" to the previous target; the searcher moves rapidly relative to the target; the target density is low; the forager does not keep memory of previous encounters; the forager has inadequate information on the area to patrol and on the target location, etc. Of course, all these characteristics provide a highly simplified representations of real foragers, yet conceptual simplifications (rather than trivializations) are often very advantageous to advance and consolidate the knowledge on a complex topic. As a matter of fact, due to the difficulty of the analytical setting (and also to mimic situations of biological interest), to develop a mathematical theory of foraging related to the Lévy flight hypothesis it is often necessary to introduce additional parameters (such as a "direct vision distance" of the predator, see page 912 in [51]) and approximations (see e.g. equations (2) and (5) in [51]). In general, in spite of several quite strong and convincing attempts to completely deduce the Lévy flight foraging hypothesis from prime principles, several important details have generated debate, see e.g. [31, 27, 13, 28] and also [26] for a review of several controversial aspects of the Lévy foraging hypothesis.

In this paper, we consider the optimal foraging strategies in several situations of biological interest, such as:

- the case in which a single target is located in the proximity of the forager's burrow,
- the case in which targets are sparsely distributed,
- the case in which a single target is located far away from the forager's burrow,
- the case in which there are two targets, one close and one far from the forager's burrow.

The optimal strategies of each of these configurations will be analyzed in light of new efficiency functionals relying also on methods from mathematical analysis and with the aid of some classical special functions.

A few comments are in order to highlight some of the main structural differences between our approach and the rather abundant existing literature on optimal animal foraging. On the one hand, the models considered here share with the existing literature several common treats, such as the assumption that the forager has no memory about the targets previously hit and that the pray has no awareness of the strategy and the movement of the predator. On the other hand, our models present significant differences with the existing literature for at least the following features:

- the forager does not restart its strategy after hitting each single target (instead, the seeker diffuses according to a Lévy type of diffusive equation, and this feature happens to be consistent with the setting of some of the existing literature, see equation (1) in [31]; similar, but different, space-fractional equations in biological environment have also been considered in view of the Caputo derivative, see equation (2.1) in [48]),

- no additional parameter related to direct vision is taken into account, no a-priori bound on step lengths is imposed, no truncation of the power law distribution is assumed (with the advantage of not endowing the problem with auxiliary and sometimes arbitrary parameters; as a counterpart of these technical and conceptual simplifications, the diffusions corresponding to infinite mean displacements are ruled out as infinite overshooting and this feature happens to be consistent with the setting of some of the existing literature, see e.g.the discussion after formula (2) in [31]),

- we will take into account time averages of foraging success (though some integrals over time were previously considered, such as in the cumulative probability in equation (6) of [31], we will specialize our analysis in detecting different optimal strategies according to the different time scales involved in the seeking process, rather than simply considering the foraging outcome at a given time),

- we will analyze in detail the role played by possibly different normalizing constants appearing when linking probabilistic models to analytical ones (typically, these constants depend[1] on the fractional exponent s, hence they may play a significant role when the objective is to optimize in s and, in general, they cannot be light-heartedly disregarded),

- we will find solutions in closed form, relying only on elementary special functions (and, since these functions, such as the Euler Gamma Function and the Riemann Zeta Function, are widely studied and already carefully implemented in all mathematical softwares, in our approach no expensive or advanced numerical simulations are needed),

- we introduce a number of new efficiency functionals whose optimization can be explicitly discussed (these functionals are inspired by, but somewhat different from, the mean first passage time adopted in [51] – in this way, we also avoid any overlap with some controversial details in the contemporary literature such as in [27, 13, 28]).

Though the arguments developed here essentially carry over to the multi-dimensional case, for the sake of simplicity (and following a consolidated tradition in mathematical biology, see e.g. [12, 31]), we stick here to dimension 1. The multi-dimensional case will be treated separately in a subsequent work, also taking into account new sets of structural parameters according to the geometry of the space and of the diffusive process.

Also, we focus here on the case of stationary targets (the case of mobile preys possibly with different velocities will be accounted for in a forthcoming work).

[1] In terms of optimization strategies, we think it would have been beneficial, for instance, to discuss more extensively the possible dependences on μ (corresponding to $1 + 2s$ here) in the right hand sides of equation (5) in [51] and equation (11) in [37], as well as the constant C in equation (4) of [49]. The explanation for the pseudo mean squared displacements in the right hand side of equation (10) of [37] could have also benefitted from further details on the possible dependence of δ and α (the latter corresponding to $2s$ here).

Notation Table	
Fourier Transform of f	$\widehat{f}(\xi) := \mathcal{F}f(\xi) := \displaystyle\int_{\mathbb{R}} f(x)e^{-2\pi ix\xi}\,dx$
Fourier Antitransform of g	$\check{g}(x) := \mathcal{F}^{-1}g(x) := \displaystyle\int_{\mathbb{R}} g(\xi)e^{2\pi ix\xi}\,d\xi$
Poisson Summation Formula	$\displaystyle\sum_{k\in\mathbb{Z}} f(x+k) = \sum_{k\in\mathbb{Z}} \widehat{f}(k)\,e^{2\pi ixk}$
Dirac Delta Function at x_0	δ_{x_0}
Integral of a continuous function ϕ against the Dirac Delta	$\displaystyle\int_{\mathbb{R}} \phi(x)\delta_{x_0}(x)\,dx := \phi(x_0)$
Fractional parameter	$s \in (0,1)$
Fractional Laplacian of u	$(-\Delta)^s u := \mathcal{F}^{-1}(|2\pi\xi|^{2s}\widehat{u})$
Gamma Function ($z \in \mathbb{C}$, $\Re(z) > 0$)	$\Gamma(z) := \displaystyle\int_0^{+\infty} \vartheta^{z-1}e^{-\vartheta}\,d\vartheta$
Euler-Mascheroni constant	$\gamma := \displaystyle\lim_{n\to\infty}\left(-\ln n + \sum_{k=1}^{n}\frac{1}{k}\right) = 0.5772156...$
Digamma Function	$\psi(z) := \dfrac{d}{dz}\ln\big(\Gamma(z)\big) = \dfrac{\Gamma'(z)}{\Gamma(z)}$
Riemann Zeta Function ($z \in \mathbb{C}$, $\Re(z) > 1$)	$\zeta(z) := \displaystyle\sum_{j=1}^{\infty}\frac{1}{j^z}$

The results obtained will detect the optimal exponent s corresponding to the most efficient foraging strategy (according to the different possible efficiency functionals). Several interesting patterns will arise. Quite often, optimal strategies are obtained in nature either by Lévy flights modeled on the inverse square law, or by the classical Brownian motion, or by some intermediate fractional values. In our discussion, all these three patterns will clearly arise and suitable bifurcation of optimal strategies will occur in dependence of the environmental parameters.

For instance, varying the time in which the search occurs or the sparseness of the targets, the optimality of the inverse square law may be lost in favor of a classical Gaussian strategy (or viceversa), and in some cases optimal values are found arbitrarily close to pessimal ones (and, conversely, pessimal values arbitrarily close to optimal ones). We think that this is a very interesting phenomenon, underlying the fact that the theoretical optimality of the strategy by itself might be not the main information to take into account for efficient search algorithms, since less ideal strategies might produce more consistent results and prove themselves to be more reliable and viable in concrete situations.

In some circumstances, we will also detect optimal fractional values of intermediate type between the inverse square law and the Gaussian. In all cases, we will develop explicit (and somewhat "elegant") representations of the efficiency functional that we introduce, thus allowing simple and effective analytic manipulations. As a byproduct, many of the environmental bifurcation parameters will be computed exactly.

The rest of the paper is organized as follows. In the forthcoming Section 2, we introduce our mathematical setting adopted in this paper, modeled on a forager randomly diffusing through a nonlocal heat equation and immobile targets with different types of distributions (see also the Notation Table for the list of the main mathematical objects and notations utilized in this paper). The different biological scenarios corresponding to these distributions of resources will be discussed in Section 3, where several efficient functionals will be optimized with respect to the diffusion exponent.

The results obtained will be also compared with the existing literature related to the Lévy foraging hypothesis.

2 Mathematical setting

We introduce now the formal mathematical that setting we work with. The setting is modeled on the fractional heat equation and goes as follows.

Let $\kappa > 0$, $s \in (0,1)$ and $u(x,t)$ be the solution[2] of

$$\begin{cases} \partial_t u = -\kappa^{2s}\,(-\Delta)^s u \quad \text{in } \mathbb{R}\times(0,+\infty), \\ u(x,0) = \delta_0(x). \end{cases} \tag{1}$$

By taking the Fourier Transform of this relation,

$$\begin{cases} \partial_t \widehat{u} = -|2\pi\kappa\xi|^{2s}\widehat{u} \quad \text{in } \mathbb{R}\times(0,+\infty), \\ \widehat{u}(x,0) = 1. \end{cases}$$

Therefore

$$\widehat{u}(\xi,t) = \exp\big(-|2\pi\kappa\xi|^{2s}t\big) \qquad \text{and} \qquad u(x,t) = \mathcal{F}^{-1}\Big(\exp\big(-|2\pi\kappa\xi|^{2s}t\big)\Big). \tag{2}$$

It is possible that the similarity (and the difference) between the expression for $\widehat{u}$ in (2) and the standard Gaussian (corresponding to $s=1$) were one of the inspiring motivations for Lévy's approach to the Central Limit Theorem in presence of infinite moments, see equation (7) in [45].

We observe that, by scaling,

$$\begin{aligned} u(x,t) &= \int_{\mathbb{R}} \exp\big(-|2\pi\kappa\xi|^{2s}t + 2\pi i x\xi\big)\,d\xi \\ &= \frac{1}{t^{\frac{1}{2s}}}\int_{\mathbb{R}} \exp\big(-|2\pi\kappa\eta|^{2s} + 2\pi i t^{-\frac{1}{2s}}x\eta\big)\,d\eta \\ &= \frac{1}{t^{\frac{1}{2s}}}\mathcal{F}^{-1}\Big(\exp\big(-|2\pi\kappa\xi|^{2s}\big)\Big)\left(\frac{x}{t^{\frac{1}{2s}}}\right) \\ &= \frac{1}{t^{\frac{1}{2s}}}u\left(\frac{x}{t^{\frac{1}{2s}}},1\right). \end{aligned} \tag{3}$$

In addition (see e.g. formula (2.30) in [1]),

$$0 \leqslant u(x,1) \leqslant \frac{C_{s,\kappa}}{1+|x|^{1+2s}}, \tag{4}$$

for some $C_{s,\kappa} > 0$ depending only on s and κ.

[2] In several occurrences in the existing literature, the Lévy exponent in biological contexts is denoted by μ. With respect to our notation, it holds that $\mu = 1+2s$.

It is also useful to recall that, according to formula (6) of [34],

$$\begin{aligned}\lim_{x\to\pm\infty}|x|^{1+2s}u(x,t) &= \lim_{x\to\pm\infty}|x|^{1+2s}\int_{\mathbb{R}} e^{-|2\pi\kappa\xi|^{2s}t}\cos(2\pi x\xi)\,d\xi\\ &= 2\lim_{x\to\pm\infty}|x|^{1+2s}\int_0^{+\infty} e^{-(2\pi\kappa\xi)^{2s}t}\cos(2\pi x\xi)\,d\xi\\ &= \frac{1}{2\pi\kappa t^{\frac{1}{2s}}}\lim_{x\to\pm\infty}|x|^{1+2s}\int_0^{+\infty} e^{-\vartheta^{2s}}\cos\left(\frac{x\vartheta}{\kappa t^{\frac{1}{2s}}}\right)\,d\xi\\ &= \frac{\kappa^{2s}\,t}{2\pi}\lim_{y\to\pm\infty}|y|^{1+2s}\int_0^{+\infty} e^{-\vartheta^{2s}}\cos(y\vartheta)\,d\xi\\ &= \frac{\kappa^{2s}\,t\,\Gamma(1+2s)\,\sin(\pi s)}{2\pi},\end{aligned} \tag{5}$$

where the substitutions $\vartheta := 2\pi\kappa\xi t^{\frac{1}{2s}}$ and $y := \frac{x}{\kappa t^{\frac{1}{2s}}}$ have been used.

3 Description of the optimal strategies in different frameworks

We introduce here the notion of value functional related to the foraging success that we aim at optimizing with respect to the parameter s.

Given a distribution of targets $p(x,t)$, the *foraging success functional* will be taken as proportional to the encounters between seekers and preys over time and therefore, given $T>0$, it takes the form

$$\iint_{\mathbb{R}\times(0,T)} p(x,t)\,u(x,t)\,dx\,dt. \tag{6}$$

We will compare this quantity, which is advantageous for the forager, with several quantities of interest which instead provide a penalization for the seeker's strategy. These terms will be *time* (thus, we will consider the amount of targets met over the time span T), a *renormalization of time* that takes into account, in some sense, the trajectory performed at a discrete level by a corresponding Lévy walker (as presented in (7) below), and the *average distance from the origin* (that is the distance of the forager "from home", as discussed in (8) below).

To present the renormalization of time, we let $s\in\left(\frac{1}{2},1\right)$ and we recall (see e.g. formula (4.6) in [1]) that the mean excursion for each time step of a discrete Lévy walker is proportional to the spacial step by a factor of the form

$$\frac{\displaystyle\sum_{j=1}^{+\infty}\frac{1}{j^{2s}}}{\displaystyle\sum_{j=1}^{+\infty}\frac{1}{j^{1+2s}}} = \frac{\zeta(2s)}{\zeta(1+2s)}.$$

Though one cannot really consider this as the distance traveled by the Lévy walker in the unit of time (due to the nonlinear dependence between space and time variables in long-jump random processes), it is suggestive to consider a possible renormalization of time of the form

$$\overline{\ell}(s,T) := \frac{T\,\zeta(2s)}{\zeta(1+2s)}. \tag{7}$$

As for the distance between the forager and its burrow (located at the origin), we consider the average displacement for $s \in \left(\frac{1}{2}, 1\right)$ given by

$$\ell(s,T) := \iint_{\mathbb{R}\times(0,T)} |x|\, u(x,t)\, dx\, dt. \tag{8}$$

We observe that this is a natural quantity to take into consideration as a penalization for long excursions to account for the forager's need to return to home. Related (but different) displacement functions were taken into account in equation (1) of [17]. A variant of this approach (that will be accounted for in a forthcoming work) consists in considering pseudo mean displacements as in equation (10) of [37], possibly also including different normalization constants.

We also recall that the quantity in (8) can be computed by using the Fourier Transform for generalized functions (see Section 3.3 in Chapter II of [19] for the main results on this topic and Section 3.9 in Chapter I of [19] for the setting of the notation related to generalized functions). Indeed, from[3] equation (2) on page 194 of [19] we know that

$$\mathcal{F}(|x|) = -\frac{1}{2\pi^2\,|\xi|^2}$$

and therefore, by Plancherel Theorem, (2) and the substitution $y := (2\pi\kappa\xi)^{2s}t$,

$$\begin{aligned}
\iint_{\mathbb{R}\times(0,T)} |x|\, u(x,t)\, dx\, dt &= \iint_{\mathbb{R}\times(0,T)} |x| \left(u(x,t) - \delta_0(x)\right) dx\, dt \\
&= -\frac{1}{2\pi^2} \iint_{\mathbb{R}\times(0,T)} \frac{\widehat{u}(\xi,t) - 1}{|\xi|^2}\, d\xi\, dt = -\frac{1}{2\pi^2} \iint_{\mathbb{R}\times(0,T)} \frac{\exp\left(-|2\pi\kappa\xi|^{2s}t\right) - 1}{|\xi|^2}\, d\xi\, dt \\
&= -\frac{1}{\pi^2} \iint_{(0,+\infty)\times(0,T)} \frac{\exp\left(-(2\pi\kappa\xi)^{2s}t\right) - 1}{\xi^2}\, d\xi\, dt \\
&= -\frac{\kappa}{\pi s} \iint_{(0,+\infty)\times(0,T)} t^{\frac{1}{2s}} \left(e^{-y} - 1\right) y^{-\frac{1}{2s}-1}\, dy\, dt.
\end{aligned}$$

In this way we obtain that

$$\begin{aligned}
\ell(s,T) &= -\frac{2\kappa\, T^{\frac{1+2s}{2s}}}{\pi\,(1+2s)} \int_0^{+\infty} \left(e^{-y} - 1\right) y^{-\frac{1}{2s}-1}\, dy \\
&= \frac{4\kappa s\, T^{\frac{1+2s}{2s}}}{\pi\,(1+2s)} \int_0^{+\infty} \left[\frac{d}{dy}\left(\frac{e^{-y}-1}{y^{\frac{1}{2s}}}\right) + \frac{e^{-y}}{y^{\frac{1}{2s}}}\right] dy \\
&= \frac{4\kappa s\, T^{\frac{1+2s}{2s}}}{\pi\,(1+2s)} \int_0^{+\infty} e^{-y}\, y^{\frac{2s-1}{2s}-1}\, dy \\
&= \frac{4\kappa s\, T^{\frac{1+2s}{2s}}}{\pi\,(1+2s)} \Gamma\left(\frac{2s-1}{2s}\right).
\end{aligned} \tag{9}$$

One of the main goals of this paper is to consider, as efficiency functional for the forager, the ratio between (6) and either the time T, or the quantity in (7), or that in (8). We stress that while T is

[3] We stress that the notation of [19] for the Fourier Transform chooses a different normalization than the one here, by defining

$$\widetilde{\mathcal{F}} f(\xi) := \int_{\mathbb{R}} f(x) e^{ix\xi}\, dx = \mathcal{F} f\left(-\frac{\xi}{2\pi}\right),$$

see formula (1) on page 153 in [19].

obviously well defined for all $s \in (0,1)$, the quantities in (7) and (8) are finite only when $s \in \left(\frac{1}{2}, 1\right)$ (formally, they can be defined to be equal to $+\infty$ when $s \in \left(0, \frac{1}{2}\right]$). The reduction of the analysis of foraging strategies in the range $s \in \left(\frac{1}{2}, 1\right)$ has been also performed elsewhere in the literature, see e.g. the discussion after formula (2) in [31] or formula (35) in [3] (it is however interesting to pursue also different approaches to incorporate conveniently modified situations in which the average jump distance is infinite, but possibly incorporating waiting times between subsequent jumps, see e.g. [30, 43, 44] and pages 34–35 in [45]).

We will also distinguish two cases of interest according to the diffusion coefficient κ in (1). Namely, we will consider the standard case in which $\kappa = 1$ (this is a classical normalization choice, see e.g. formula (1) in [31]), as well as the case in which κ depends on s via the relation

$$\kappa = \left(-\frac{\cos(\pi s)\Gamma(-2s)}{\zeta(1+2s)} \right)^{\frac{1}{2s}} =: \kappa_s. \tag{10}$$

This form of the diffusion coefficient is the one emerging in the formal passage to the continuous limit of a random Lévy walker in the discrete lattice $h\mathbb{Z}$ for time steps $\tau = h^{2s}$, since, in this setting,

$$\begin{aligned}
\frac{u(x,t+\tau)-u(x,t)}{\tau} &= \left(\sum_{k\in\mathbb{Z}\setminus\{0\}} \frac{1}{|k|^{1+2s}} \right)^{-1} \sum_{k\in\mathbb{Z}\setminus\{0\}} \frac{u(x+hk,t)-u(x,t)}{h^{2s}|k|^{1+2s}} \\
&= \left(2\sum_{k=1}^{+\infty} \frac{1}{k^{1+2s}} \right)^{-1} \sum_{k=1}^{+\infty} \frac{u(x+hk,t)+u(x-hk,t)-2u(x,t)}{h^{2s}k^{1+2s}} \\
&\simeq \frac{1}{2\zeta(1+2s)} \int_0^{+\infty} \frac{u(x+y,t)+u(x-y,t)-2u(x,t)}{y^{1+2s}}\, dy,
\end{aligned}$$

where we have approximated a Riemann sum with the corresponding integral. Thus setting $v_{y,t}(x) := u(x+y,t)$, and noticing that

$$\widehat{v}_{y,t}(\xi) = \int_{\mathbb{R}} u(x+y,t)e^{-2\pi i x\xi}\, dx = e^{2\pi i y\xi} \int_{\mathbb{R}} u(z,t)e^{-2\pi i z\xi}\, dz = e^{2\pi i y\xi}\, \widehat{u}(\xi,t),$$

we see that, in the formal limit,

$$\begin{aligned}
\partial_t u(x,t) &= \frac{1}{2\zeta(1+2s)} \mathcal{F}^{-1}\left(\int_0^{+\infty} \frac{e^{2\pi i y\xi} + e^{-2\pi i y\xi} - 2}{y^{1+2s}}\, dy\, \widehat{u}(\xi,t) \right) \\
&= -\frac{1}{\zeta(1+2s)} \mathcal{F}^{-1}\left(\int_0^{+\infty} \frac{1-\cos(2\pi y\xi)}{y^{1+2s}}\, dy\, \widehat{u}(\xi,t) \right) \\
&= -\frac{(2\pi)^{2s}}{\zeta(1+2s)} \int_0^{+\infty} \frac{1-\cos z}{z^{1+2s}}\, dz\, \mathcal{F}^{-1}\left(|\xi|^{2s}\, \widehat{u}(\xi,t) \right) \\
&= \frac{\cos(\pi s)\Gamma(-2s)}{\zeta(1+2s)} \mathcal{F}^{-1}\left(|2\pi\xi|^{2s}\, \widehat{u}(\xi,t) \right) \\
&= \frac{\cos(\pi s)\Gamma(-2s)}{\zeta(1+2s)} (-\Delta)^s u(x,t)
\end{aligned}$$

see e.g. the appendix in [15] for the computation of the latter constant (which is negative), and this justifies (10).

Moreover, using the functional equation (40.5) in [35] (and, as customary, adopting the notation that extends the Riemann Zeta Function by analytic continuation), we can simplify the expression for κ_s in (10) and get

$$\kappa_s = \frac{1}{2\pi}\left(-\frac{1}{2\zeta(-2s)}\right)^{\frac{1}{2s}}. \tag{11}$$

3.1 Single prey at the origin

We now consider the case of a single target located at the origin. In this case, the distribution of prey can be written as

$$p_0(x) = \delta_0(x).$$

We observe that, by (2),

$$\begin{aligned}\int_{\mathbb{R}} p_0(x)u(x,t)\,dx = u(0,t) = \mathcal{F}^{-1}\big(\widehat{u}(\cdot,t)\big)(0,t) &= \int_{\mathbb{R}} \exp\big(-|2\pi\kappa\xi|^{2s}t\big)\,d\xi \\ &= 2\int_0^{+\infty} \exp\big(-(2\pi\kappa\xi)^{2s}t\big)\,d\xi.\end{aligned} \tag{12}$$

Also, making use of the change of variable $\vartheta := (2\pi\kappa\xi)^{2s}t$, we see that

$$2\int_0^{+\infty} \exp\big(-(2\pi\kappa\xi)^{2s}t\big)\,d\xi = \frac{1}{2\pi\kappa\, s\, t^{\frac{1}{2s}}}\int_0^{+\infty} \vartheta^{\frac{1}{2s}-1}e^{-\vartheta}\,d\vartheta = \frac{1}{2\pi\kappa\, s\, t^{\frac{1}{2s}}}\,\Gamma\left(\frac{1}{2s}\right). \tag{13}$$

Thus, in the notation of (6), using (12) and (13), the foraging success functional for a single target located at the origin takes the form, for $s \in \big(\frac{1}{2}, 1\big)$,

$$\Phi_0(s;\kappa,T) := \iint_{\mathbb{R}\times(0,T)} p_0(x)u(x,t)\,dx\,dt = \int_0^T \frac{1}{2\pi\kappa\, s\, t^{\frac{1}{2s}}}\,\Gamma\left(\frac{1}{2s}\right)\,dt = \frac{T^{\frac{2s-1}{2s}}}{\pi\kappa\,(2s-1)}\Gamma\left(\frac{1}{2s}\right), \tag{14}$$

and takes value equal to $+\infty$ when $s \in \big(0, \frac{1}{2}\big]$. Hence, recalling (7), (9) and (11), we consider the utility functionals defined for $s \in \big(\frac{1}{2}, 1\big)$ given by

$$\begin{aligned}
\mathcal{E}_1(s;T) &:= \frac{\Phi_0(s;1,T)}{T} = \frac{1}{\pi\, T^{\frac{1}{2s}}\,(2s-1)}\Gamma\left(\frac{1}{2s}\right),\\
\mathcal{E}_2(s;T) &:= \frac{\Phi_0(s;\kappa_s,T)}{T} = \frac{2\big(-2\zeta(-2s)\big)^{\frac{1}{2s}}}{T^{\frac{1}{2s}}\,(2s-1)}\Gamma\left(\frac{1}{2s}\right),\\
\mathcal{E}_3(s;T) &:= \frac{\Phi_0(s;1,T)}{\overline{\ell}(s,T)} = \frac{\zeta(1+2s)}{\pi\, T^{\frac{1}{2s}}\,(2s-1)\,\zeta(2s)}\Gamma\left(\frac{1}{2s}\right),\\
\mathcal{E}_4(s;T) &:= \frac{\Phi_0(s;\kappa_s,T)}{\overline{\ell}(s,T)} = \frac{\zeta(1+2s)2\big(-2\zeta(-2s)\big)^{\frac{1}{2s}}}{T^{\frac{1}{2s}}\,(2s-1)\,\zeta(2s)}\Gamma\left(\frac{1}{2s}\right),\\
\mathcal{E}_5(s;T) &:= \frac{\Phi_0(s;1,T)}{\ell(s,T)} = \frac{(1+2s)\,\Gamma\left(\frac{1}{2s}\right)}{4s\,(2s-1)\,T^{\frac{1}{s}}\,\Gamma\left(\frac{2s-1}{2s}\right)}\\
\text{and}\qquad \mathcal{E}_6(s;T) &:= \frac{\Phi_0(s;\kappa_s,T)}{\ell(s,T)} = \frac{\pi^2\big(-2\zeta(-2s)\big)^{\frac{1}{s}}\,(1+2s)\,\Gamma\left(\frac{1}{2s}\right)}{s\,(2s-1)\,T^{\frac{1}{s}}\,\Gamma\left(\frac{2s-1}{2s}\right)}.
\end{aligned} \tag{15}$$

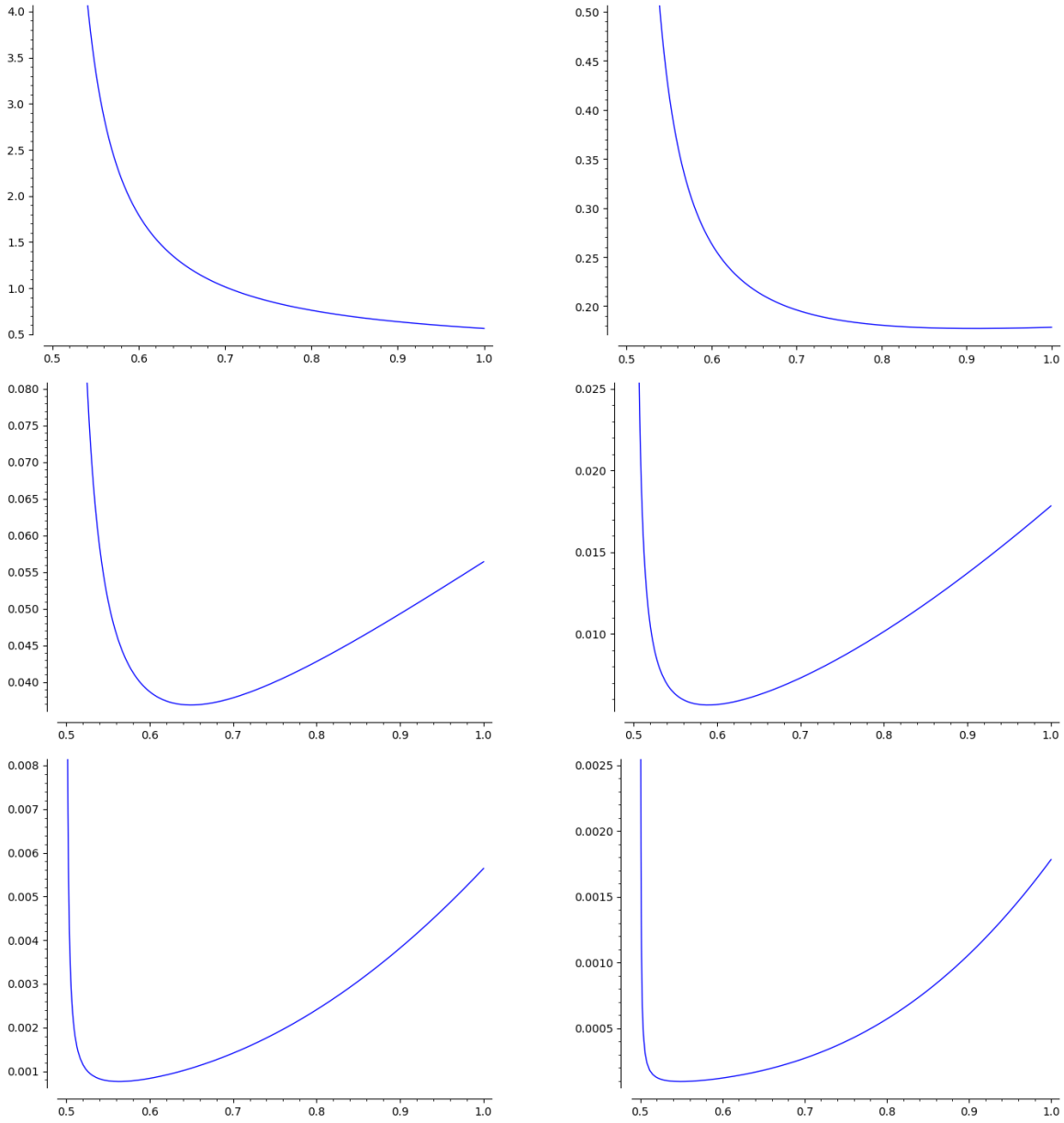

Figure 1: *Plot of* $\left(\frac{1}{2},1\right) \ni s \mapsto \mathcal{E}_1(s;T)$ *for* $T = 10^j$, $j \in \{0,\ldots,5\}$.

We observe that

$$\lim_{s \searrow 1/2} \mathcal{E}_1(s;T) = +\infty,$$

therefore, for every $T > 0$.

the supremum of the utility functional $\left(\frac{1}{2},1\right) \mapsto \mathcal{E}_1(s;T)$ is uniquely attained at $s = \frac{1}{2}$. (16)

We recall that the value $s = \frac{1}{2}$ occurs often in optimal foraging problems, as an ideal balance between intensive search and longer (hence energetically more expensive) movements, both in terms of real world data (such as for atlantic cods, see e.g. Figure 1d in [46], jackals, see e.g. [4], wandering albatrosses, see e.g. Figure 1 in [25], deers, see e.g. Figure 2(a) in [29], bees, see [42], fruit flies, see [40], and also Amazonian farmers searching for nuts, see Figure 3(b.09) in [39], etc.) and of

theoretical optimization (see [51, 12]). Interestingly, it also occurs in patterns generated by human ecology (such as distances between campsites, see Figure 1 in [11]). With respect to these data, the statement in (16) can be seen as a confirmation of the most common paradigm in the Lévy foraging hypothesis. On the other hand, the qualitative behaviour of $\mathcal{E}_1(s;T)$ changes dramatically for large intervals of time: indeed, as hinted by Figure 1 (that plots $\mathcal{E}_1(\cdot;T)$ for $T \in \{1, 10, 10^2, 10^3, 10^4, 10^5\}$), we have that

$$\begin{aligned} &\text{for large } T, \text{ the utility functional } \left(\frac{1}{2}, 1\right) \mapsto \mathcal{E}_1(s;T) \\ &\text{has a unique minimum at some point } s_T \text{ such that} \\ &\lim_{T\to+\infty} s_T = \frac{1}{2} \qquad \text{and} \qquad \lim_{T\to+\infty} \mathcal{E}_1(s_T;T) = 0. \end{aligned} \tag{17}$$

This is an interesting phenomenon, showing that the optimality at $s = \frac{1}{2}$ may become "unstable" and depends on the time span in which the phenomenon is observed, allowing a sudden switch between the optimal (but somehow unreliable) Lévy foraging pattern and the less ideal (but somehow more secure) classical Brownian motion strategy.

It is suggestive to compare this phenomenon to other occurrences in which Lévy flights with $s = \frac{1}{2}$ should theoretically provide the optimal seeking strategy but they coexist with another possible notion of foraging optimization related to Brownian walks, see e.g. the end of page 9 in [12].

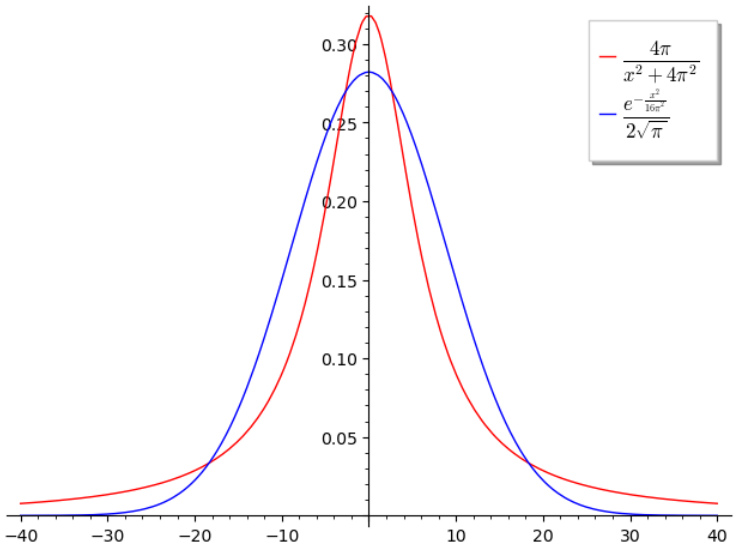

Figure 2: *Plot of $x \mapsto u(x,1)$ with $\kappa = 1$ corresponding to $s = \frac{1}{2}$ (in magenta) and to $s = 1$ (in blue).*

A heuristic explanation for the statement in (17) can be given in terms of the behaviour of the function u (with $\kappa = 1$) at the origin and at infinity in dependence of the parameter s. Indeed, while the usual paradigm is to relate small values of s to long excursions of the traveller, this general notion has sometimes to be revised according to the specific mathematical model taken into account in the diffusive strategy of the forager, since, on the one hand, solutions of equation (1) corresponding to lower values of s do present a fatter tail distribution, but, on the other hand, due to the loss of the regularizing effect of the diffusive operator for small s, they also present a more prominent mass at

the origin: see e.g. Figure 2 in which one can compare solutions at time $t = 1$ corresponding to $s = \frac{1}{2}$ and $s = 1$. Thus, the balance of these two apparently contrasting features may provide advantageous foragers' strategies for small values of s also in presence of proximate preys (not due to the long range excursion induced by the fat tail of the distribution, but rather due to the distribution peak at the origin produced by the less regularizing effect of a lower order operator). With respect to this observation, in view of the scaling properties of the equation (see (3)), the prominent role of the peak at the origin occurs for small times, while it becomes less significant for larger times. This somehow explains why the Lévy flights corresponding to $s = \frac{1}{2}$ are, in principle, more favorable than the classical Brownian motion, but this effect may become less relevant and rather insecure for very long time spans. It is suggestive to investigate whether the interplay between optimal but unstable strategies with suboptimal but safer ones may play a role in the appearance in nature of composite correlated random walks and in the biological approximation of Lévy walks as an innate composite correlated random walks, see [7, 38].

It is also interesting to compare with biological situations in which a predominance of classical random walks coexists with patterns close to a theoretical optimum of $s = \frac{1}{2}$, see e.g. Figure 4 in [22].

We stress that the phenomenon described in (17) relies on the ideal assumption that the target is modelled as a "material point" (thus any arbitrarily small diffusion of the forager misses the resource) and is a byproduct of a memory-less search strategy (see e.g. [18] for a discussion of memory-enhanced foraging strategies).

The statement in (17) can be checked analytically as detailed in Appendix A.1.

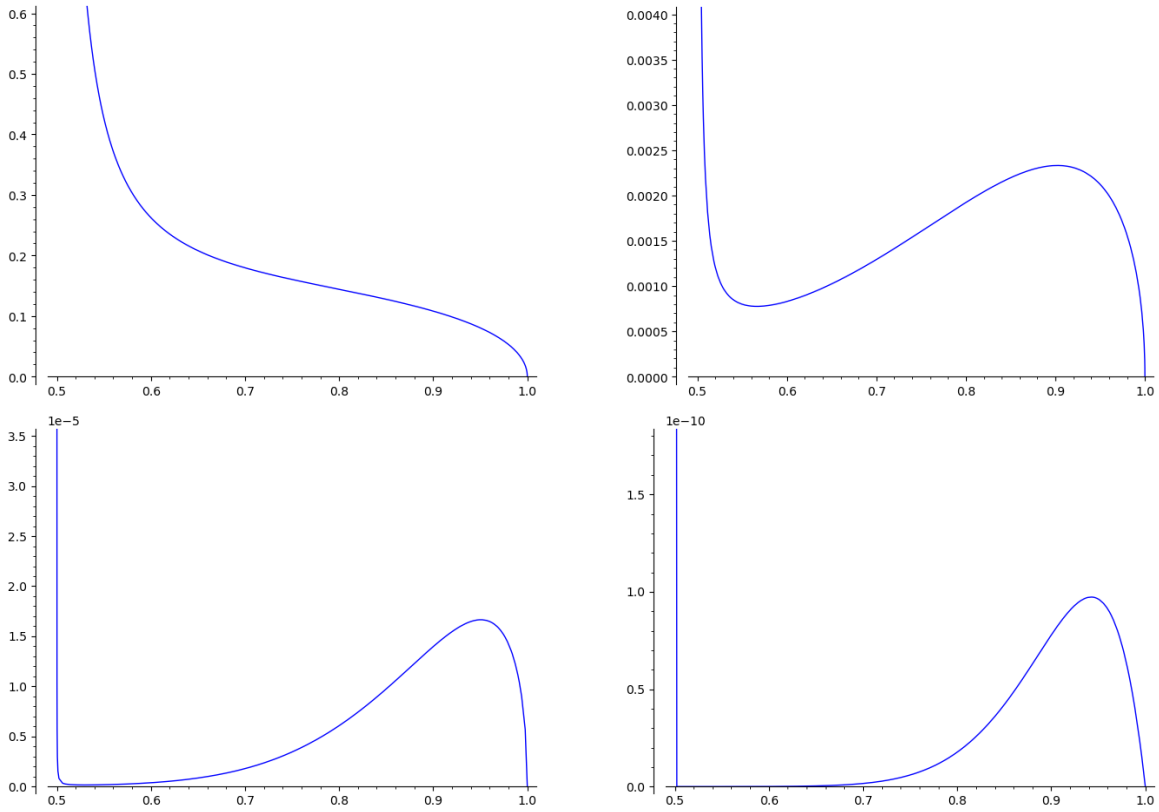

Figure 3: *Plot of* $(\frac{1}{2}, 1) \ni s \mapsto \mathcal{E}_2(s; T)$ *for* $T = 10^j$, $j \in \{1, 4, 8, 16\}$.

We also have that

$$\lim_{s \searrow 1/2} \mathcal{E}_2(s;T) = +\infty$$

and, in view of the divergence of the Gamma Functions at negative integers,

$$\lim_{s \nearrow 1} \mathcal{E}_2(s;T) = 0.$$

These equations show that, for every $T > 0$

$$\begin{aligned} &\text{the supremum of the utility functional } \left(\frac{1}{2}, 1\right) \mapsto \mathcal{E}_2(s;T) \text{ is uniquely attained at } s = \frac{1}{2} \\ &\text{and the infimum is uniquely attained at } s = 1, \end{aligned} \tag{18}$$

which in turn suggests a very strong advantage for the Lévy strategy compared to the Poisson one. On the other hand, for long time spans, the pattern in (18) shows a significant instability, as sketched in Figure 3, which depicts the map $\mathcal{E}_2(\cdot;T)$ for $T \in \{10, 10^4, 10^8, 10^{16}\}$. As a result,

$$\begin{aligned} &\text{for large } T, \text{ the utility functional } \left(\frac{1}{2}, 1\right) \mapsto \mathcal{E}_2(s;T) \\ &\text{has a local minimum at some point } s_T \text{ such that} \\ &\lim_{T \to +\infty} s_T = \frac{1}{2} \qquad \text{and} \qquad \lim_{T \to +\infty} \mathcal{E}_2(s_T;T) = 0, \\ &\text{and a local maximum at some point } S_T \text{ such that } \lim_{T \to +\infty} S_T = 1. \end{aligned} \tag{19}$$

The statement in (19) can be checked analytically as detailed in Appendix A.2.

Interesting patterns having a theoretical (but unstable for large time) optimum at $s = \frac{1}{2}$ with a stabilizing option at $s = 1$ are exhibited by the utility functionals $\mathcal{E}_5$ and $\mathcal{E}_6$: see Figure 4 for the sketch of $\mathcal{E}_5(\cdot;T)$ (notice the pattern change between $T = 1.1$ and $T = 1.5$ and the development of an interior maximum at $T = 1.3$) and Figure 5 for the sketch of $\mathcal{E}_6(\cdot;T)$. We also stress that, for a given T, the values of $\mathcal{E}_5$ and $\mathcal{E}_6$ remain finite (differently from the cases of $\mathcal{E}_1$ and $\mathcal{E}_2$).

The cases of the utility functionals $\mathcal{E}_3$ and $\mathcal{E}_4$ are instead surprisingly different. Indeed, Figure 6 hints that $\mathcal{E}_3$ is monotone decreasing with a supremum at $s = \frac{1}{2}$ when $T \leqslant 1.5$, but then its monotonicity behavior changes when $T \geqslant 1.6$ and develops a supremum at $s = 1$ when $T \geqslant 1.7$. In this case, even the theoretical optimality at $s = \frac{1}{2}$ is lost for large times and additionally the switch between Lévy and Poisson optimal strategy occurs with a rather abrupt transition with respect to the parameter T.

The functional $\mathcal{E}_4$ exhibits a different and interesting pattern, as highlighted in Figure 7: in this case the system shows a sudden change of optimality occurring between $T = 2$ and $T = 3$: it appears indeed that the Lévy foraging for $s = \frac{1}{2}$ is optimal when $T \leqslant 2$, but when $T \geqslant 3$ a new

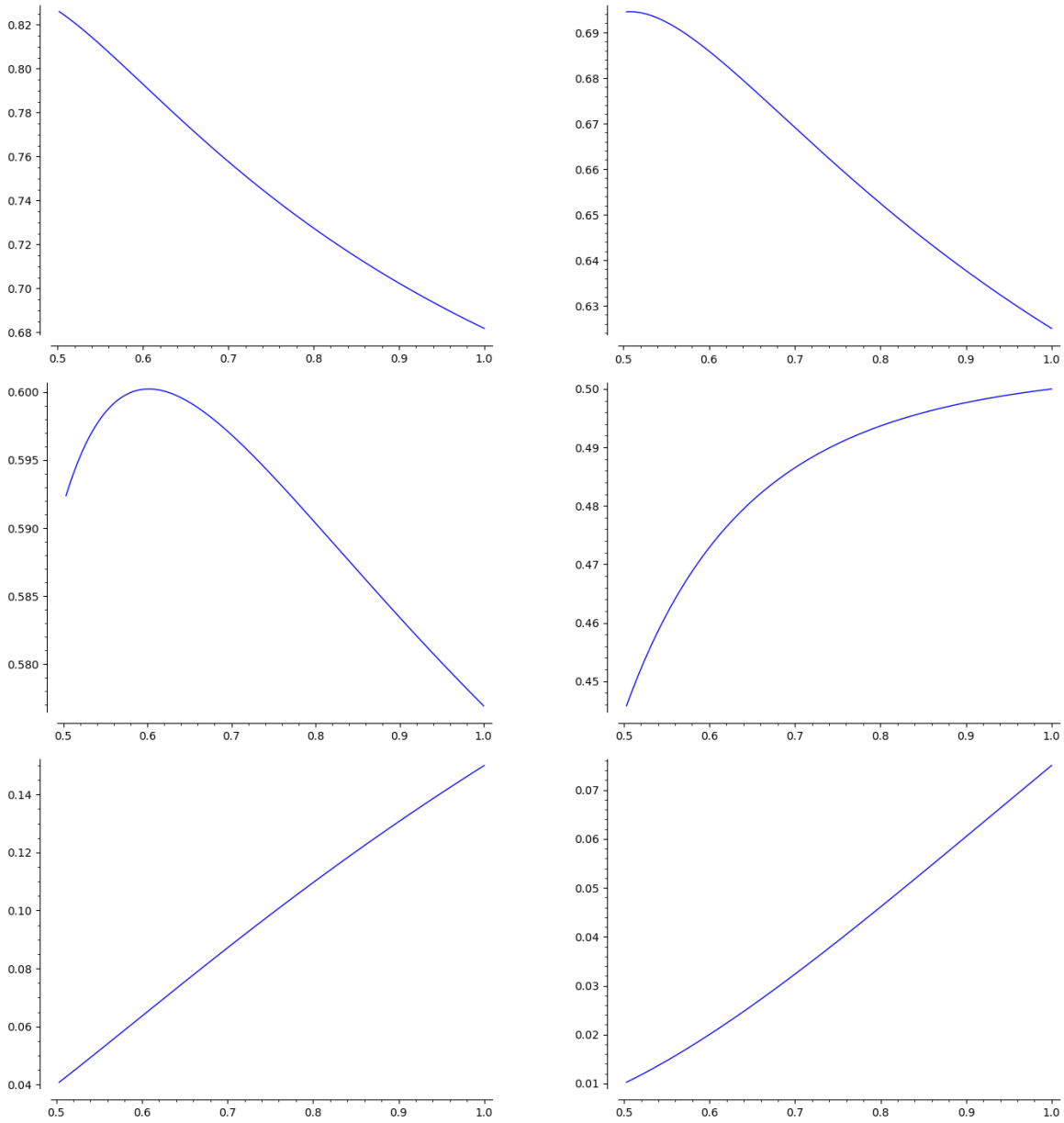

Figure 4: *Plot of* $(\frac{1}{2}, 1) \ni s \mapsto \mathcal{E}_5(s;T)$ *for* $T \in \{1.1, 1.2, 1.3, 1.5, 5, 10\}$.

optimal strategy for a different fractional exponent s arises (with this new optimal exponent moving towards $s = 1$ as T becomes large).

As a matter of fact, we can detect analytically this bifurcation phenomenon and find an explicit value for the critical T by the following analytic argument. We use the notation $\epsilon := 2s - 1$ according to which we have that

$$(2s-1)\zeta(2s) = \epsilon\zeta(1+\epsilon) = 1 + \gamma\epsilon + o(\epsilon)$$

and therefore

$$\begin{aligned}
\mathcal{E}_4(s;T) &= \frac{2\,\zeta(2+\epsilon)\,\left(-2\zeta(-\epsilon-1)\right)^{\frac{1}{1+\epsilon}}}{T^{\frac{1}{1+\epsilon}}\,(1+\epsilon\gamma+o(\epsilon))}\,\Gamma\left(\frac{1}{1+\epsilon}\right) \\
&= \frac{2\,(\zeta(2)+\zeta'(2)\epsilon+o(\epsilon))\,\left(-2\zeta(-1)+2\zeta'(-1)\epsilon+o(\epsilon)\right)^{\frac{1}{1+\epsilon}}}{(T-T\ln T\epsilon+o(\epsilon))(1+\gamma\epsilon+o(\epsilon))}\,(1+\gamma\epsilon+o(\epsilon))
\end{aligned}$$

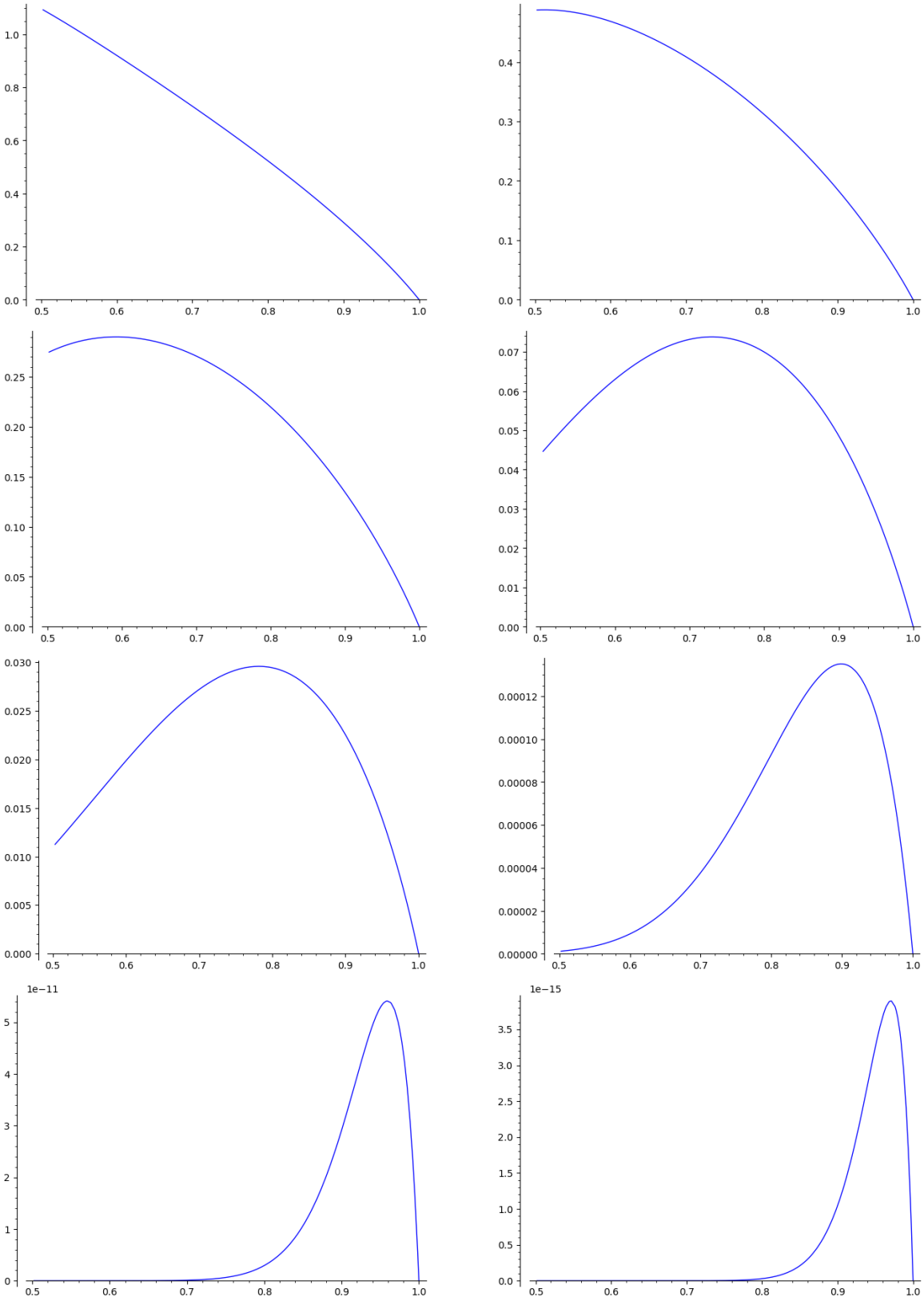

Figure 5: *Plot of* $\left(\frac{1}{2},1\right) \ni s \mapsto \mathcal{E}_6(s;T)$ *for* $T \in \{1, 1.5, 2, 5, 10, 10^3, 10^9, 10^{13}\}$.

$$= \quad 2\left(\frac{\pi^2}{6} + \zeta'(2)\epsilon + o(\epsilon)\right)\left(\frac{1}{6} + \frac{1}{6}\ln 6\,\epsilon + 2\zeta'(-1)\epsilon + o(\epsilon)\right)\left(\frac{1}{T} + \frac{\ln T}{T}\epsilon + o(\epsilon)\right) + o(\epsilon)$$

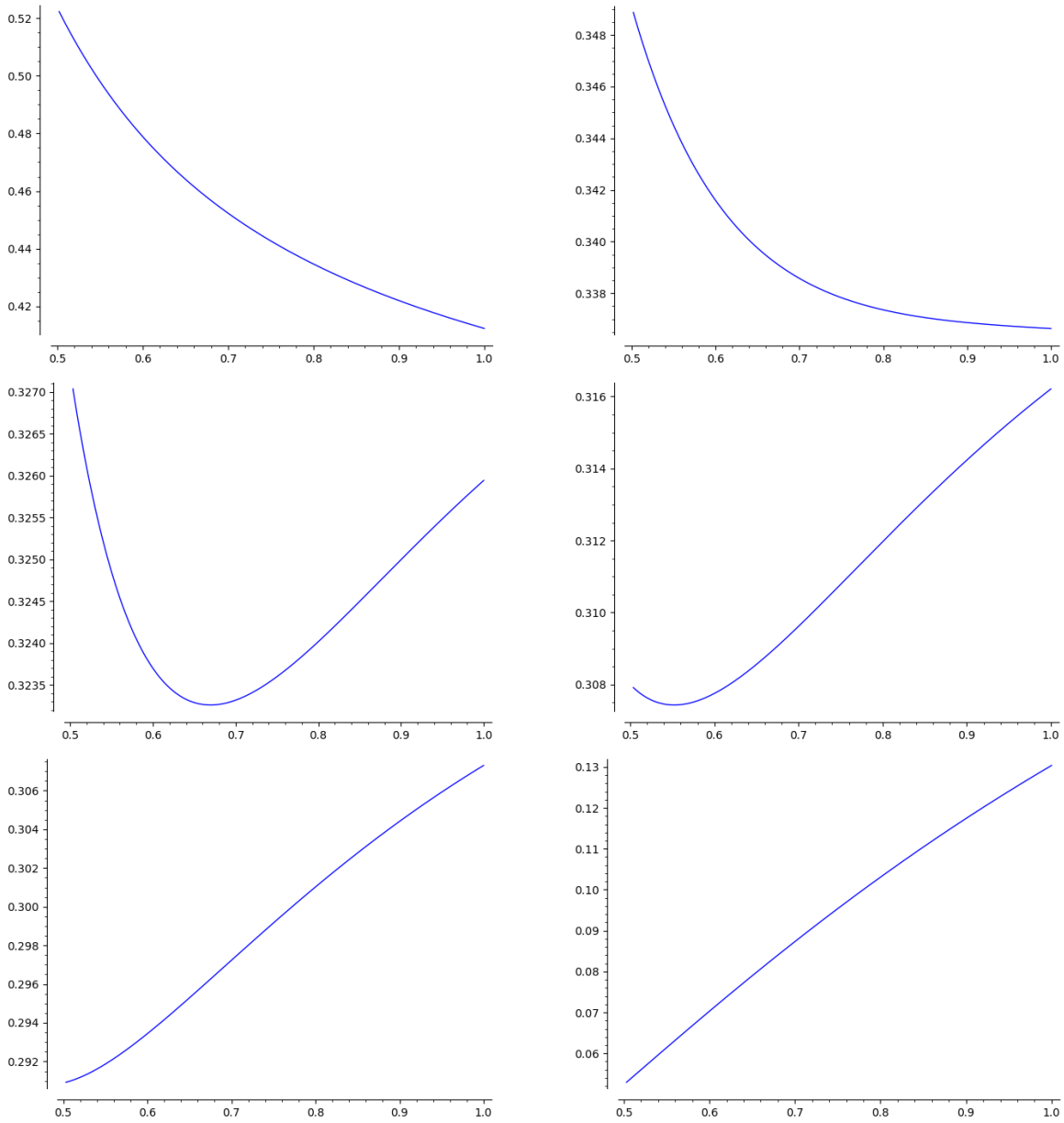

Figure 6: *Plot of* $\left(\frac{1}{2},1\right) \ni s \mapsto \mathcal{E}_3(s;T)$ *for* $T \in \{1, 1.5, 1.6, 1.7, 1.8, 10\}$.

$$= \frac{\pi^2}{18\,T} + 2\epsilon\left(\frac{\pi^2}{36\,T}\ln T + \frac{\pi^2}{36\,T}\ln 6 + \frac{\pi^2}{3\,T}\zeta'(-1) + \frac{\zeta'(2)}{6\,T}\right) + o(\epsilon)$$

This yields that

$$\frac{9T}{\pi^2}\frac{d\mathcal{E}_4}{ds}\left(\frac{1}{2};T\right) = \ln T + \ln 6 + 12\zeta'(-1) + \frac{6}{\pi^2}\zeta'(2)$$

and this quantity is positive (respectively, negative) when $T > T_\star$ (respectively, when $T < T_\star$), where

$$T_\star := \exp\left(-\ln 6 - 12\zeta'(-1) - \frac{6}{\pi^2}\zeta'(2)\right) = 2.145248182...$$

and, as a result, when $T > T_\star$ the inverse square law $s = \frac{1}{2}$ cannot maximize $\mathcal{E}_4$ and values of s even slightly larger than $\frac{1}{2}$ provide greater values of such an efficiency functional.

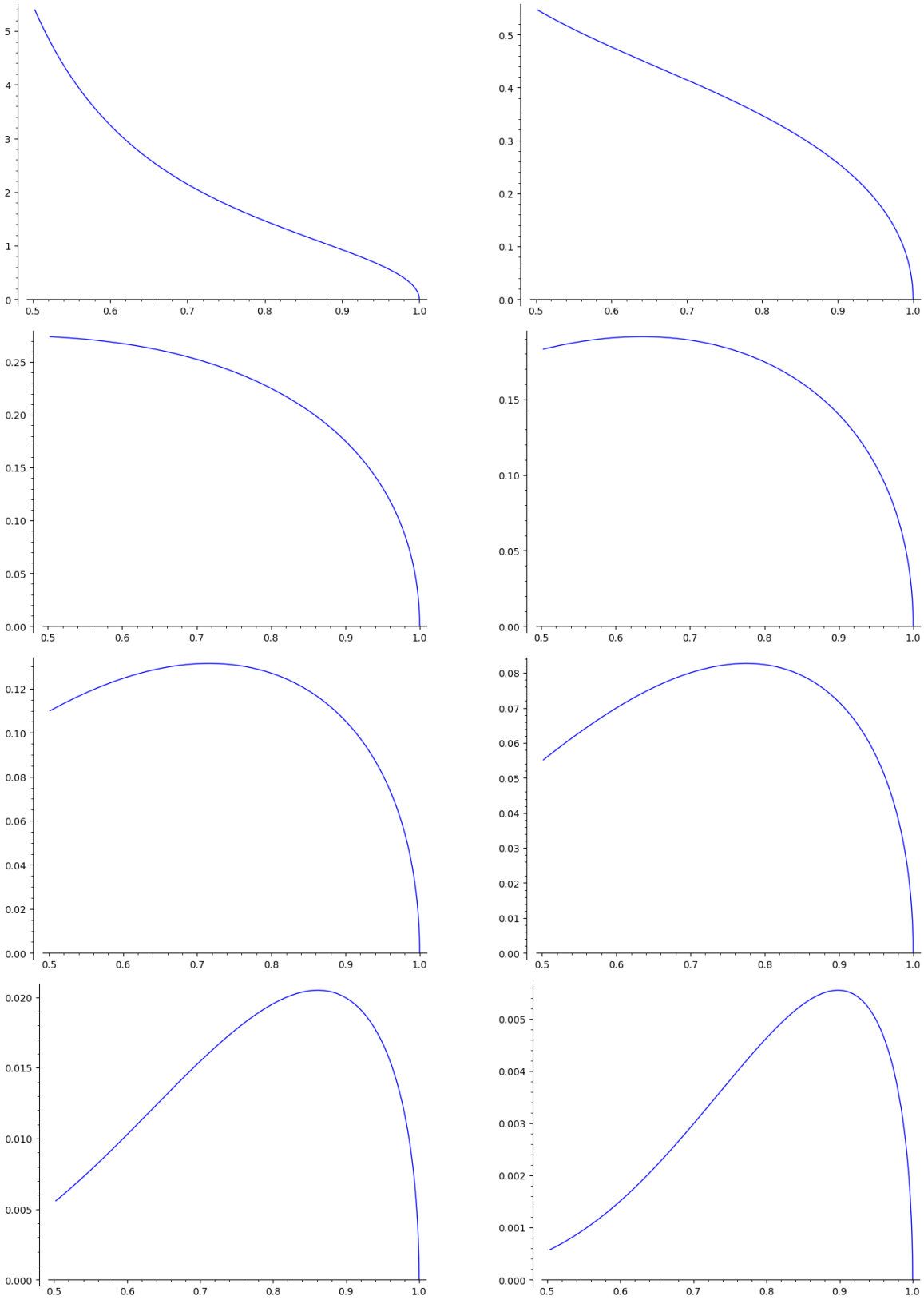

Figure 7: *Plot of* $\left(\frac{1}{2}, 1\right) \ni s \mapsto \mathcal{E}_4(s;T)$ *for* $T \in \{0.1, 1, 2, 3, 5, 10, 100, 1000\}$.

3.2 Preys on a sparse lattice

Now we take into consideration a set of targets displayed in the lattice $\lambda\mathbb{Z}$, for some $\lambda > 0$, and we consider the asymptotics related to large values of λ, corresponding to the case of sparse preys. To this end, we consider the target distribution

$$p(x) := \sum_{k\in\mathbb{Z}} \delta_{\lambda k}(x).$$

We observe that

$$\int_{\mathbb{R}} p(x)u(x,t)\,dx = \sum_{k\in\mathbb{Z}} u(\lambda k,t) = \sum_{k\in\mathbb{Z}} u_\lambda(k,t) \tag{20}$$

where

$$u_\lambda(x,t) := u(\lambda x,t).$$

By (3) and (4),

$$\begin{aligned}(1+|x|^{1+2s})|u_\lambda(x,t)| &= (1+|x|^{1+2s})|u(\lambda x,t)| = \frac{1+|x|^{1+2s}}{t^{\frac{1}{2s}}} u\left(\frac{\lambda x}{t^{\frac{1}{2s}}},1\right)\\ &\leqslant \frac{C\,(1+|x|^{1+2s})}{t^{\frac{1}{2s}}\left(1+\left|\frac{\lambda x}{t^{\frac{1}{2s}}}\right|^{1+2s}\right)} \leqslant C_{s,\lambda,t},\end{aligned} \tag{21}$$

for some $C_{s,\lambda,t}\in(0,+\infty)$.

Moreover, by (2),

$$\begin{aligned}\widehat{u}_\lambda(\xi,t) &= \int_{\mathbb{R}} u(\lambda x,t)e^{-2\pi i x\xi}\,dx = \frac{1}{\lambda}\int_{\mathbb{R}} u(y,t)e^{-2\pi i\lambda^{-1}y\xi}\,dy\\ &= \frac{1}{\lambda}\widehat{u}\left(\frac{\xi}{\lambda},t\right) = \frac{1}{\lambda}\exp\left(-\frac{|2\pi\kappa\xi|^{2s}t}{\lambda^{2s}}\right)\end{aligned}$$

and accordingly

$$(1+|\xi|^{1+2s})|\widehat{u}_\lambda(\xi,t)| = \frac{1+|\xi|^{1+2s}}{\lambda}\exp\left(-\frac{|2\pi\kappa\xi|^{2s}t}{\lambda^{2s}}\right) \leqslant \widetilde{C}_{s,\lambda,t},$$

for some $\widetilde{C}_{s,\lambda,t}\in(0,+\infty)$.

In view of this estimate and (21), for a given $t>0$ we can use the Poisson Summation Formula on u_λ (see e.g. formula (4.4.2) and Theorem 4.4.2 in [33]) and, in light of (20), conclude that

$$\int_{\mathbb{R}} p(x)u(x,t)\,dx = \sum_{k\in\mathbb{Z}} u_\lambda(k) = \sum_{k\in\mathbb{Z}} \widehat{u}_\lambda(k) = \frac{1}{\lambda}\sum_{k\in\mathbb{Z}}\exp\left(-\frac{|2\pi k|^{2s}t}{\lambda^{2s}}\right).$$

For large λ, we can consider the latter term as a Riemann sum, therefore, using polar coordinates,

$$\int_{\mathbb{R}} p(x)u(x,t)\,dx \simeq \int_{\mathbb{R}}\exp\left(-|2\pi y|^{2s}t\right)\,dy = 2\int_0^{+\infty}\exp\left(-(2\pi\rho)^{2s}t\right)\,d\rho.$$

Thus, recalling (6), (13) and (14), we can consider, for large λ, the foraging success functional

$$\Phi(s) := \iint_{\mathbb{R}\times(0,T)} p(x)u(x,t)\,dx\,dt \simeq \frac{1}{2\pi s}\,\Gamma\left(\frac{1}{2s}\right)\int_0^T \frac{dt}{t^{\frac{1}{2s}}} = \frac{T^{\frac{2s-1}{2s}}}{\pi(2s-1)}\,\Gamma\left(\frac{1}{2s}\right) = \Phi_0(s;1,T).$$

The case of a sparse distribution of targets is therefore reduced to that of a single prey at the origin and, since the optimizers discussed in Section 3.1 were isolated and nondegenerate, the analysis provided in Section 3.1 for a single prey gives asymptotic information to the case of sparsely distributed targets when λ is sufficiently large.

3.3 Remote single prey

Now we consider the case of a single target located far away from the initial position of the seeker. For this, given $L > 0$, let

$$p_L(x) := \delta_L(x).$$

For $T > 0$, in view of (6), we consider the foraging success functional

$$\Phi_{L,T}(s;\kappa) := \iint_{\mathbb{R}\times(0,T)} p_L(x)u(x,t)\,dx\,dt = \int_0^T u(L,t)\,dt$$

By (5), for large L,

$$L^{1+2s}\,\Phi_{L,T}(s;\kappa) \simeq \int_0^T \frac{\kappa^{2s}\,t\,\Gamma(1+2s)\,\sin(\pi s)}{2\pi}\,dt = \frac{\kappa^{2s}\,T^2\,\Gamma(1+2s)\,\sin(\pi s)}{4\pi}.$$

Thus, in the lines of (15), we set

$$\widetilde{\Phi}_{L,T}(s;\kappa) := \frac{\kappa^{2s}\,T^2\,\Gamma(1+2s)\,\sin(\pi s)}{4\pi L^{1+2s}},$$

we notice that

$$\Phi_{L,T}(s;\kappa) \simeq \widetilde{\Phi}_{L,T}(s;\kappa) \tag{22}$$

for large L, and we discuss the optimization of the utility functionals[4]

$$\begin{aligned}
\mathcal{G}_1(s;L,T) &:= \frac{\widetilde{\Phi}_{L,T}(s;1)}{T} = \frac{T\,\Gamma(1+2s)\,\sin(\pi s)}{4\pi\,L^{1+2s}},\\
\mathcal{G}_2(s;L,T) &:= \frac{\widetilde{\Phi}_{L,T}(s;\kappa_s)}{T} = -\frac{T\Gamma(-2s)\,\Gamma(1+2s)\,\sin(2\pi s)}{8\pi\,L^{1+2s}\,\zeta(1+2s)} = \frac{T}{8L^{1+2s}\,\zeta(2s+1)},\\
\mathcal{G}_3(s;L,T) &:= \frac{\widetilde{\Phi}_{L,T}(s;1)}{\overline{\ell}(s,T)} = \frac{T\,\zeta(1+2s)\,\Gamma(1+2s)\,\sin(\pi s)}{4\pi L^{1+2s}\,\zeta(2s)},\\
\mathcal{G}_4(s;L,T) &:= \frac{\widetilde{\Phi}_{L,T}(s;\kappa_s)}{\overline{\ell}(s,T)} = -\frac{T\,\Gamma(-2s)\,\Gamma(1+2s)\,\sin(2\pi s)}{8\pi L^{1+2s}\,\zeta(2s)} = \frac{T}{8L^{1+2s}\zeta(2s)},\\
\mathcal{G}_5(s;L,T) &:= \frac{\widetilde{\Phi}_{L,T}(s;1)}{\ell(s,T)} = \frac{T^{\frac{2s-1}{2s}}\,\Gamma(2+2s)\,\sin(\pi s)}{16L^{1+2s}\,\Gamma\left(\frac{2s-1}{2s}\right)}\\
\text{and}\qquad \mathcal{G}_6(s;L,T) &:= \frac{\widetilde{\Phi}_{L,T}(s;\kappa_s)}{\ell(s,T)} = \left(\frac{-1}{2^{1+2s}\pi^{2s}\zeta(-2s)}\right)^{\frac{2s-1}{2s}}\frac{T^{\frac{2s-1}{2s}}\,\Gamma(2+2s)\,\sin(\pi s)}{16L^{1+2s}\,\Gamma\left(\frac{2s-1}{2s}\right)}.
\end{aligned} \tag{23}$$

We point out that the final time T does not play any role in the optimization in s of the value functionals $\mathcal{G}_1$, $\mathcal{G}_2$, $\mathcal{G}_3$ and $\mathcal{G}_4$ in (23). We also stress that the biological meaning of the efficiency functionals in (23) only occurs for large values of $L > 0$, due to the asymptotics in (22), nevertheless it is interesting to study those functionals for all values of L also to detect bifurcation phenomena with respect to this parameter that depend only on the final analytic formulation and not on their initial construction.

[4]The final expressions for $\mathcal{G}_2$ and $\mathcal{G}_4$ are due to Euler's reflection formula

$$\Gamma(1-z)\Gamma(z) = \frac{\pi}{\sin(\pi z)} \qquad \text{for all } z \in \mathbb{R}\setminus\mathbb{Z}.$$

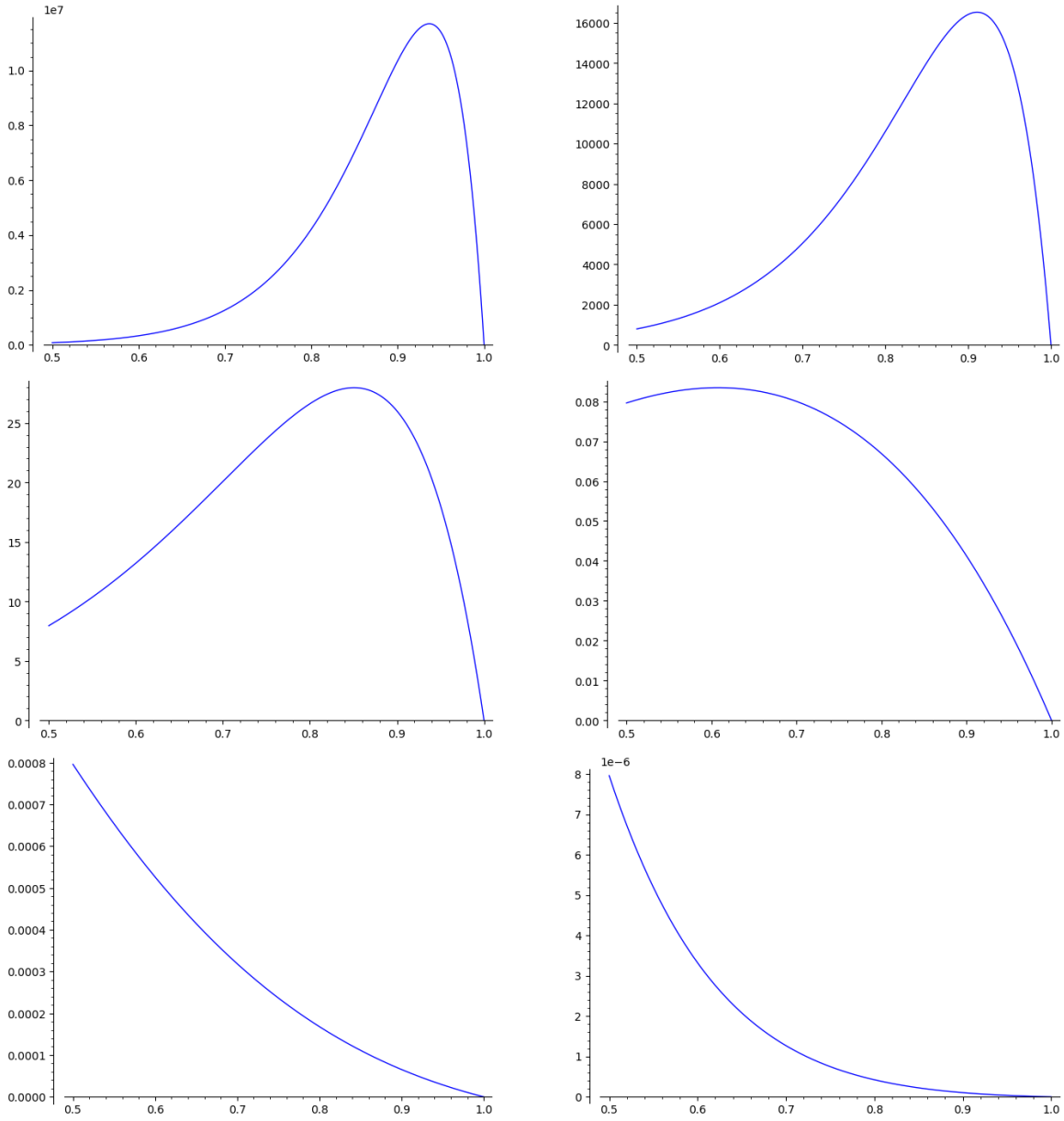

Figure 8: *Plot of* $\left(\frac{1}{2},1\right) \ni s \mapsto \mathcal{G}_1(s;L,T)$ *(say, when* $T=1$*) for* $L=10^j$*, with* $j \in \{-3,\dots,2\}$.

A plot of $\mathcal{G}_1$ is given in Figure 8, where one can appreciate that for small values of L the optimal exponent is close (but not equal) to 1 (consistently with the idea that if the prey is close to the starting point of the predator the best seeking strategy is close to that of local type), while for large values of L the optimum is provided by the inverse square law $s=\frac{1}{2}$.

The functional $\mathcal{G}_2$ also shows an interesting bifurcation diagram plotted in Figure 9: also in this framework preys located close to the origin favor local diffusive strategies (optimized in this case for $s=1$) and when L becomes larger an larger the optimal exponent moves to the left till becomes $s=\frac{1}{2}$. The similarities and differences between Figures 8 and 9 highlight how different normalization choices in the model can affect optimal strategies: note indeed that the only difference

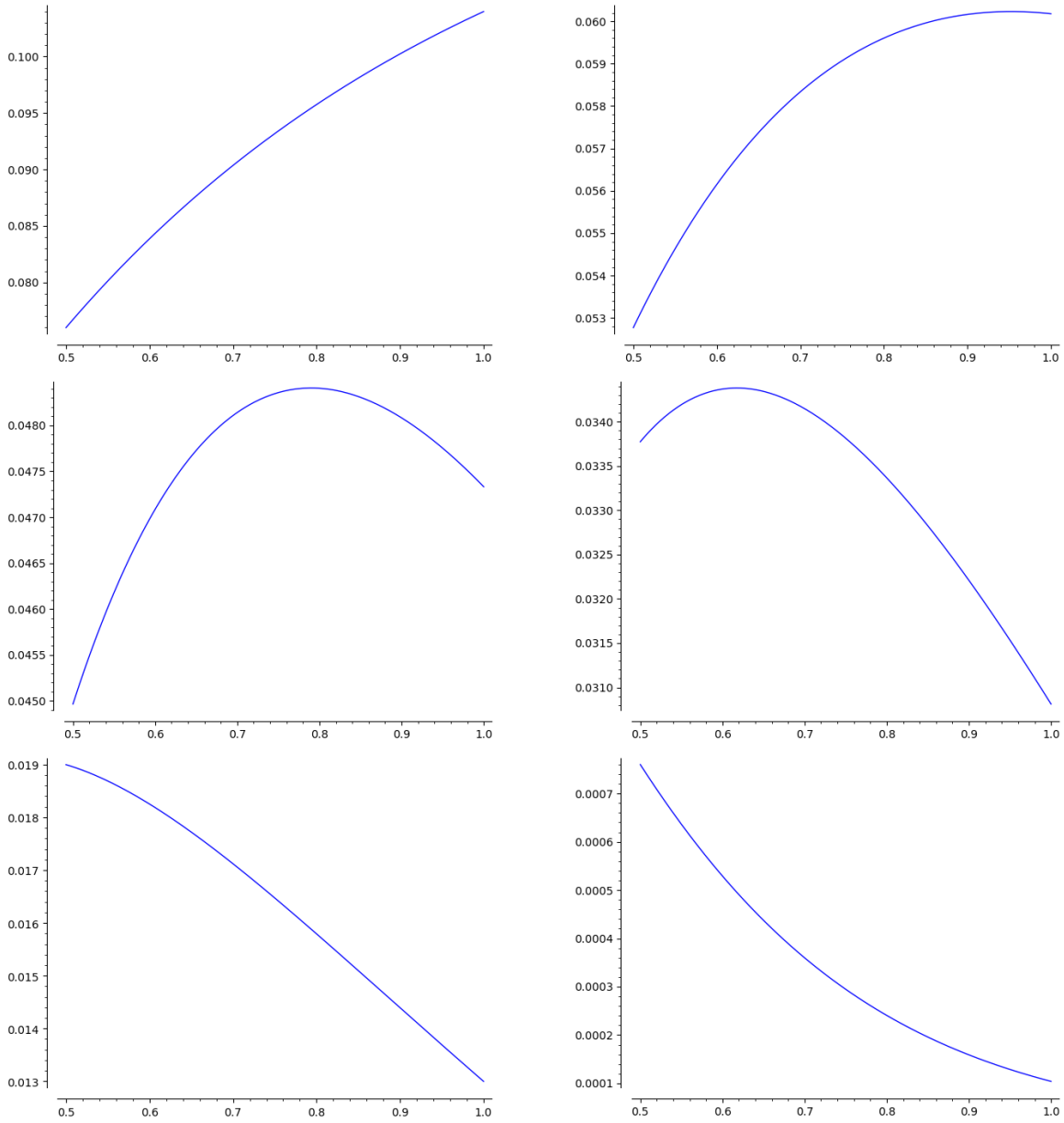

Figure 9: *Plot of* $\left(\frac{1}{2}, 1\right) \ni s \mapsto \mathcal{G}_2(s; L, T)$ *(say, when* $T = 1$*) for* $L \in \{1, 1.2, 1.3, 1.5, 2, 10\}$.

between $\mathcal{G}_1$ and $\mathcal{G}_2$ lies in the way the diffusion coefficient κ is modeled on the basis of the underlying random process. The sensitivity of the optimization strategies with respect to these normalizing constants seems to be not investigated in the current literature and it produces in Figures 8 and 9 a different outcome on the optimality of the Gaussian exponent $s = 1$; this interesting difference is induced by the analytical observation that $\mathcal{G}_1(1; L, T) = 0 < \mathcal{G}_2(1; L, T)$.

As for the functional $\mathcal{G}_3$, plots for different values of L are given in Figure 10. Interestingly, on the one hand, both the inverse square law $s = \frac{1}{2}$ and the Gaussian law $s = 1$ are minima for the functional for every T and L; on the other hand, for very sparse targets (corresponding to large values

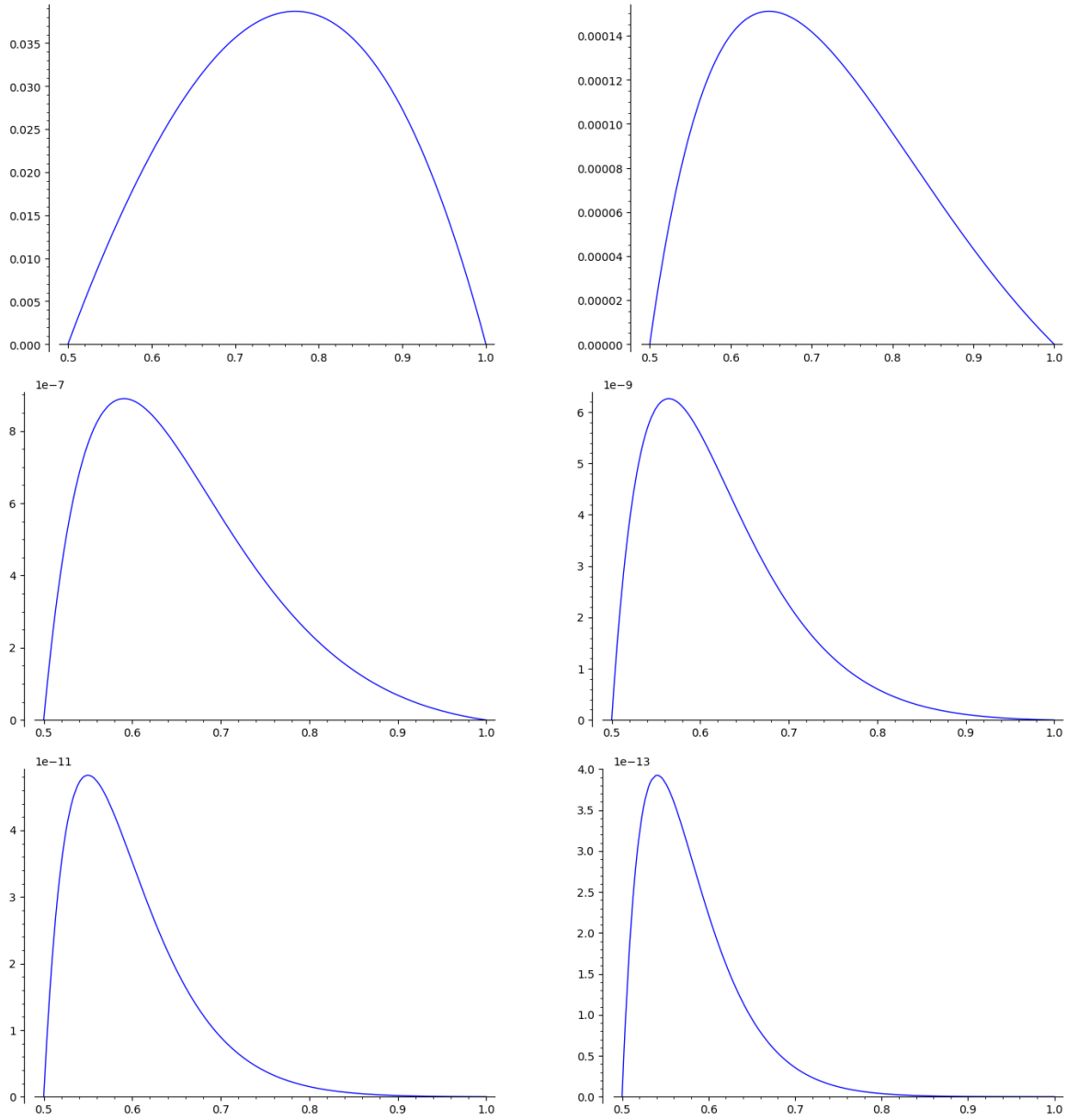

Figure 10: *Plot of* $\left(\frac{1}{2},1\right) \ni s \mapsto \mathcal{G}_3(s;L,T)$ *for* $T=1$ *and* $L=10^j$, $j \in \{0,\dots,5\}$.

of L),

$$\text{the optimal foraging strategy for } \mathcal{G}_3(s;L,T) \text{ is uniquely attained at some } s_L \text{ such that } \lim_{L\to+\infty} s_L = \frac{1}{2}. \tag{24}$$

This can also be proved analytically, see Appendix A.3.

The graph of the functional $\mathcal{G}_4$ is instead plotted in Figure 11: notice that for $L \leqslant 1.7$ this functional is increasing and attains its maximum for the Gaussian strategy $s=1$, but for $L \geqslant 2$ the functional $\mathcal{G}_4$ develops an interior maximum. More precisely, as proved analytically in Appendix A.4,

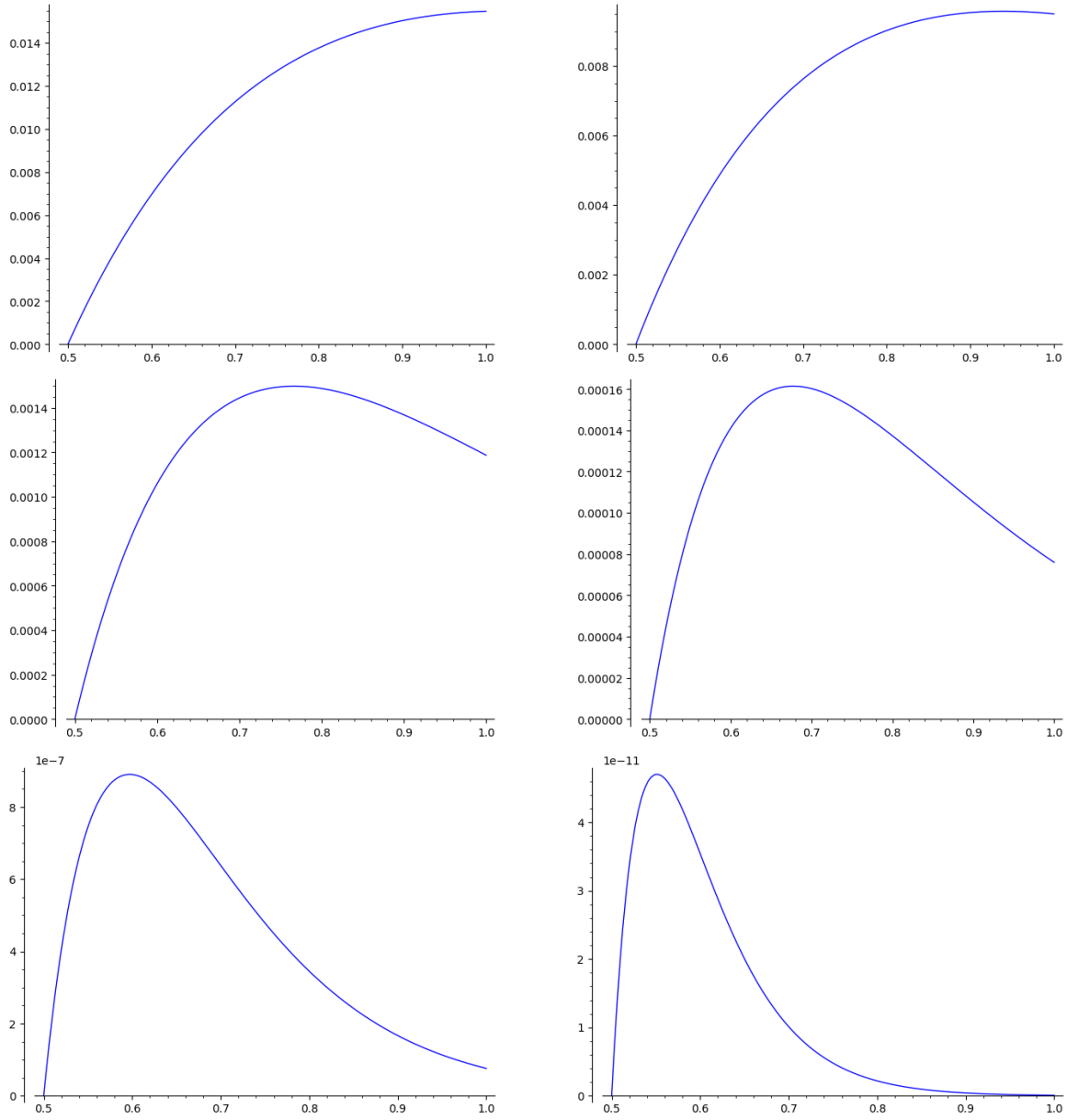

Figure 11: *Plot of* $(\frac{1}{2}, 1) \ni s \mapsto \mathcal{G}_4(s; L, T)$ *for* $T = 1$ *and* $L \in \{1.7, 2, 4, 10, 100, 10000\}$.

setting

$$L^\star := \exp\left(-\frac{\zeta'(2)}{\zeta(2)}\right) = 1.768198... \tag{25}$$

we have that

$$\begin{aligned} &\text{if } L \leqslant L^\star \text{ the optimal foraging strategy for } \mathcal{G}_4(s; L, T) \text{ is uniquely attained at } s = 1, \\ &\text{while if } L > L^\star \text{ the optimal foraging strategy for } \mathcal{G}_4(s; L, T) \text{ is uniquely attained} \\ &\text{at some } s_L \in \left(\frac{1}{2}, 1\right) \text{ such that } \lim_{L \to +\infty} s_L = \frac{1}{2}. \end{aligned} \tag{26}$$

Therefore, for larger and larger values of $L > L^\star$, the optimal strategy for $\mathcal{G}_4$ is getting closer and closer to the inverse power law distribution induced by $s = \frac{1}{2}$.

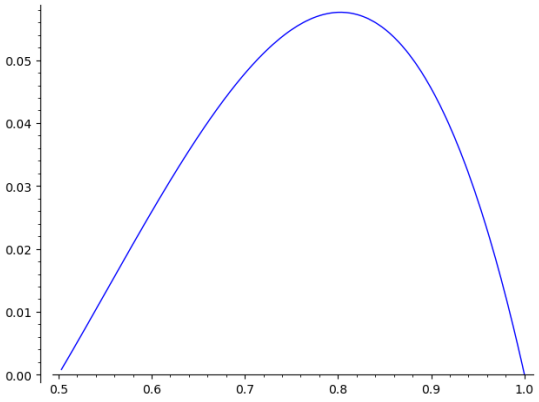

Figure 12: *Plot of* $\left(\frac{1}{2},1\right) \ni s \mapsto \mathcal{G}_5(s;L,T)$ *for* $L = T^{\frac{2s-1}{2s(1+2s)}}$.

The cases of $\mathcal{G}_5$ and $\mathcal{G}_6$ are quite sophisticated, since their optimization strategies depend both on the final time T and on the scantness of the targets modeled by L. In the special situation in which $L = T^{\frac{2s-1}{2s(1+2s)}}$ these value functionals do not depend on L and T and they are plotted in Figures 12 and 13, respectively.

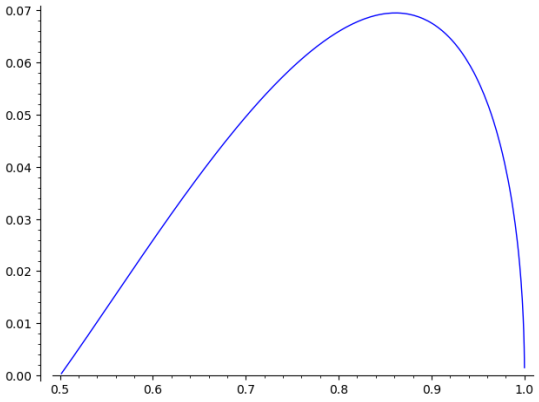

Figure 13: *Plot of* $\left(\frac{1}{2},1\right) \ni s \mapsto \mathcal{G}_6(s;L,T)$ *for* $L = T^{\frac{2s-1}{2s(1+2s)}}$.

In particular, it appears that when $L = T^{\frac{2s-1}{2s(1+2s)}}$ the functional $\mathcal{G}_5$ is maximized in proximity of $s = 0.80261...$ and $\mathcal{G}_6$ in proximity of $s = 0.861187...$: in spite of the rather arbitrary choice relating T and L in Figures 12 and 13, it is suggestive to compare these optimal intermediate values between the inverse square power law distribution and the Gaussian one with the ones observed experimentally for some blue sharks (see e.g. Figure 1b in [23] which would correspond to $s = 0.73$), basking sharks and bigeye tunas (see e.g. Figures 1b and 1c in [46] which would correspond to $s = 0.7$). See also the red curves in Figures 2, 4 and 6 of [31] (which corresponds to $s \simeq 0.75$). It is also interesting to compare these values with the simulation data of some swarm dynamics (corresponding to $s = 0.745$, see Figure 3 in [41]). Of course, we are not aiming here at precisely reconstructing the quantitative results arising in specific real-world experiments, but we think it is an interesting feature that even the very simplified situation that we describe may lead to optimal values of s which are somewhat intermediate between $s = \frac{1}{2}$ and $s = 1$.

3.4 Prey at the origin and remote prey

We now consider the case of two targets, one located "at home" at the origin and another far away at a given distance $L > 0$. This corresponds to a prey distribution of the form

$$p_{0,L}(x) := \delta_0(x) + \delta_L(x).$$

Since the foraging success functional in (6) is linear with respect to the target distribution, the analysis of this case reduces to the superposition of the value functionals introduced in (15) and (23): thus, in the above notation, we define

$$\mathcal{H}_j(s; L, T) := \mathcal{E}_j(s; T) + \mathcal{G}_j(s; L, T) \qquad \text{for } j \in \{1, \dots, 6\}$$

and we find that

$$\mathcal{H}_1(s; L, T) = \frac{1}{\pi\, T^{\frac{1}{2s}}\,(2s-1)}\Gamma\left(\frac{1}{2s}\right) + \frac{T\,\Gamma(1+2s)\,\sin(\pi s)}{4\pi\, L^{1+2s}},$$

$$\mathcal{H}_2(s; L, T) = \frac{2\big(-2\zeta(-2s)\big)^{\frac{1}{2s}}}{T^{\frac{1}{2s}}\,(2s-1)}\Gamma\left(\frac{1}{2s}\right) + \frac{T}{8L^{1+2s}\,\zeta(2s+1)},$$

$$\mathcal{H}_3(s; L, T) = \frac{\zeta(1+2s)}{\pi\, T^{\frac{1}{2s}}\,(2s-1)\,\zeta(2s)}\Gamma\left(\frac{1}{2s}\right) + \frac{T\,\zeta(1+2s)\,\Gamma(1+2s)\,\sin(\pi s)}{4\pi L^{1+2s}\,\zeta(2s)},$$

$$\mathcal{H}_4(s; L, T) = \frac{\zeta(1+2s)2\big(-2\zeta(-2s)\big)^{\frac{1}{2s}}}{T^{\frac{1}{2s}}\,(2s-1)\,\zeta(2s)}\Gamma\left(\frac{1}{2s}\right) + \frac{T}{8L^{1+2s}\zeta(2s)},$$

$$\mathcal{H}_5(s; L, T) = \frac{(1+2s)\,\Gamma\left(\frac{1}{2s}\right)}{4s\,(2s-1)\,T^{\frac{1}{s}}\,\Gamma\left(\frac{2s-1}{2s}\right)} + \frac{T^{\frac{2s-1}{2s}}\,\Gamma(2+2s)\,\sin(\pi s)}{16L^{1+2s}\,\Gamma\left(\frac{2s-1}{2s}\right)}$$

and

$$\mathcal{H}_6(s; L, T) = \frac{\pi^2\big(-2\zeta(-2s)\big)^{\frac{1}{s}}\,(1+2s)\,\Gamma\left(\frac{1}{2s}\right)}{s\,(2s-1)\,T^{\frac{1}{s}}\,\Gamma\left(\frac{2s-1}{2s}\right)} + \left(\frac{-1}{2^{1+2s}\pi^{2s}\,\zeta(-2s)}\right)^{\frac{2s-1}{2s}} \frac{T^{\frac{2s-1}{2s}}\,\Gamma(2+2s)\,\sin(\pi s)}{16L^{1+2s}\,\Gamma\left(\frac{2s-1}{2s}\right)}.$$

We point out that in all the above value functionals, the second term becomes predominant for large values of T, hence the long time analysis for $\mathcal{H}_j$ boils down to the one developed for $\mathcal{G}_j$ in Section 3.3 (this is consistent with the idea that for long times the forager has drifted away from its initial location). Similarly, small values of T reduce the analysis of $\mathcal{H}_j$ to the one developed for $\mathcal{E}_j$ in Section 3.1 (consistently with the ansatz that for small times the forager will exploit the targets in the vicinity of its burrow).

Instead, when $T = 1$ both the terms in $\mathcal{H}_j$ contribute to the optimization of $\mathcal{H}_j$ and the corresponding plots (when also $L = 1$) are given in Figure 14, showing an optimal foraging strategy corresponding to $s = \frac{1}{2}$ in these specific situations.

Acknowledgments

SD and EV are members of INdAM and AustMS. Supported by the Australian Laureate Fellowship FL190100081 "Minimal surfaces, free boundaries and partial differential equations" and by the Australian Research Council DECRA DE180100957 "PDEs, free boundaries and applications".

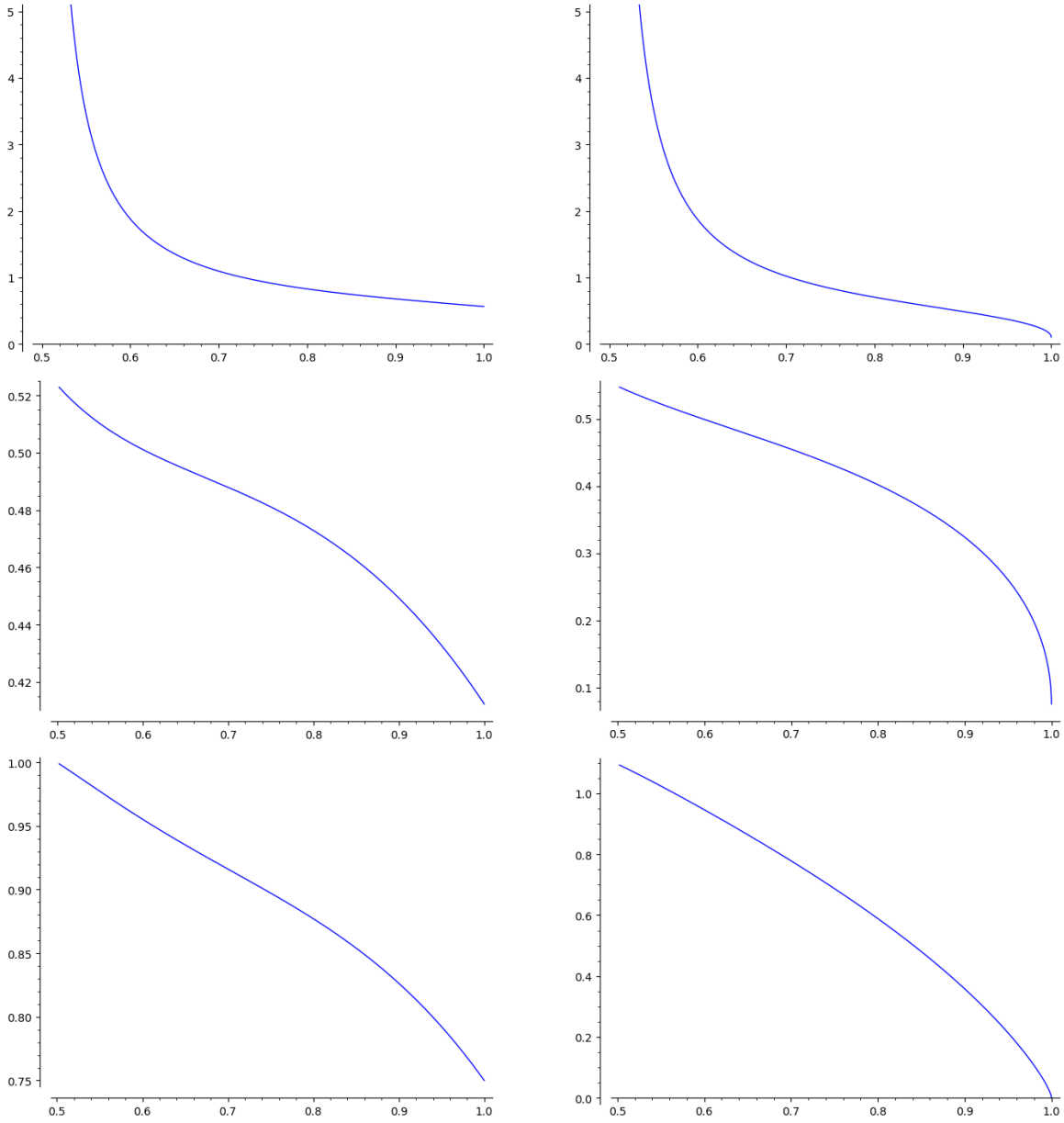

Figure 14: *Plot of* $(\frac{1}{2}, 1) \ni s \mapsto \mathcal{H}_j(s; L, T)$ *for* $T = 1 = L$ *and* $j \in \{1, \ldots, 6\}$.

A Appendices

A.1 Analytical verification of (17)

Let

$$c(s;T) := \frac{1}{2\pi T^{\frac{1}{2s}}(2s-1)^2 s^2}\,\Gamma\left(\frac{1}{2s}\right) \tag{27}$$

and notice that

$$\begin{aligned} \frac{d}{ds}c(s;T) &= \left(\frac{\ln T}{2s^2} - \frac{4}{2s-1} - \frac{2}{s}\right) c(s;T) - \frac{1}{4\pi T^{\frac{1}{2s}}(2s-1)^2 s^4}\,\Gamma'\left(\frac{1}{2s}\right) \\ &= \left(\frac{\ln T}{2s^2} - \frac{4}{2s-1} - \frac{2}{s} - \frac{1}{2s^2}\psi\left(\frac{1}{2s}\right)\right) c(s;T). \end{aligned} \tag{28}$$

Moreover, by (15),

$$\mathcal{E}_1(s;T) = 2s^2(2s-1)\,c(s;T) \tag{29}$$

and therefore

$$\begin{aligned} \frac{d}{ds}\mathcal{E}_1(s;T) &= \left(4s(2s-1)+4s^2\right)c(s;T) + 2s^2(2s-1)\frac{d}{ds}c(s;T) \\ &= \left((2s-1)\ln T - 4s^2 - (2s-1)\psi\left(\frac{1}{2s}\right)\right)c(s;T). \end{aligned} \tag{30}$$

Now we define

$$Z(x) := \sum_{k=1}^{\infty}\left(\frac{1}{k+x}-\frac{1}{k}\right) \tag{31}$$

and (see Chapter 10 in [2]) we find that

$$\psi(x) = -\gamma - \frac{1}{x} - \sum_{k=1}^{+\infty}\left(\frac{1}{k+x}-\frac{1}{k}\right) = -\gamma - \frac{1}{x} - Z(x). \tag{32}$$

Accordingly, we can rewrite equation (30) as

$$\frac{d}{ds}\mathcal{E}_1(s;T) = \left((2s-1)\ln T + (2s-1)\gamma - 2s + (2s-1)\,Z\left(\frac{1}{2s}\right)\right)c(s;T). \tag{33}$$

Moreover, since $s \in \left(\frac{1}{2},1\right)$, we have that $\frac{1}{2s} \in \left(\frac{1}{2},1\right)$ and therefore, for each $k \geqslant 1$,

$$\frac{1}{k+\frac{1}{2s}} - \frac{1}{k} \geqslant \frac{1}{k+1} - \frac{1}{k} = -\frac{1}{k(k+1)} \geqslant -\frac{1}{k^2}.$$

As a result,

$$-1 < -\frac{\pi^2}{12} = -\frac{1}{2}\sum_{k=1}^{\infty}\frac{1}{k^2} \leqslant \frac{1}{2}Z\left(\frac{1}{2s}\right) \leqslant 0. \tag{34}$$

We now define the function

$$f(s) := \Big((2s-1)\ln T + (2s-1)\gamma - 2s - 2(2s-1)\Big)\,c(s;T) \tag{35}$$

and we deduce from (33) and (34) that

$$f(s) \leqslant \frac{d}{ds}\mathcal{E}_1(s;T). \tag{36}$$

For T large enough such that $\ln T + \gamma \geqslant 3$, let

$$\overline{s}_T := \frac{1}{2}\left(\frac{\ln T + \gamma - 2}{\ln T + \gamma - 3}\right) \tag{37}$$

and observe that

$$f(s) \geqslant 0 \text{ if and only if } s \in (\overline{s}_T, 1)\,. \tag{38}$$

Recalling (15), we observe that

$$\lim_{s\to\frac{1}{2}} \mathcal{E}_1(s,T) = +\infty.$$

This limit together with (38) and (36) imply that

$$\text{the map } \left(\tfrac{1}{2},1\right) \ni s \mapsto \mathcal{E}_1(s;T) \text{ attains its minimum somewhere in the interval } \left(\tfrac{1}{2},\overline{s}_T\right). \tag{39}$$

Furthermore, by (28) and (30),

$$\begin{aligned}
&\frac{d^2}{ds^2}\mathcal{E}_1(s;T)\\
&= \left(2\ln T - 8s - 2\psi\left(\frac{1}{2s}\right) + \frac{2s-1}{2s^2}\psi'\left(\frac{1}{2s}\right)\right) c(s;T)\\
&\quad + \left((2s-1)\ln T - 4s^2 - (2s-1)\psi\left(\frac{1}{2s}\right)\right)\frac{d}{ds}c(s;T)\\
&= \left[\left(2\ln T - 8s - 2\psi\left(\frac{1}{2s}\right) + \frac{2s-1}{2s^2}\psi'\left(\frac{1}{2s}\right)\right)\right.\\
&\quad \left. + \left((2s-1)\ln T - 4s^2 - (2s-1)\psi\left(\frac{1}{2s}\right)\right)\left(\frac{\ln T}{2s^2} - \frac{4}{2s-1} - \frac{2}{s} - \frac{1}{2s^2}\psi\left(\frac{1}{2s}\right)\right)\right] c(s;T)\\
&\geqslant \left[\frac{(2s-1)\ln^2 T}{2s^2} - \left(4 + \frac{2(2s-1)}{s} + \frac{2s-1}{s^2}\psi\left(\frac{1}{2s}\right)\right)\ln T + \frac{16s^2}{2s-1} - C\right] c(s;T)
\end{aligned}$$

for some $C > 0$ independent on T.

Hence, setting $A := \frac{\sqrt{2s-1}\,\ln T}{\sqrt{2}\,s}$ and $B := \frac{4s}{\sqrt{2s-1}}$, and noticing that

$$4\sqrt{2}\,\ln T = 2AB \leqslant A^2 + B^2 = \frac{(2s-1)\ln^2 T}{2s^2} + \frac{16s^2}{2s-1},$$

we conclude that

$$\frac{d^2}{ds^2}\mathcal{E}_1(s;T) \geqslant \left[\left(4\sqrt{2} - 4 - \frac{2(2s-1)}{s} - \frac{2s-1}{s^2}\psi\left(\frac{1}{2s}\right)\right)\ln T - C\right] c(s;T). \tag{40}$$

Now, recalling (32) and (34),

$$\begin{aligned}
&4\sqrt{2} - 4 - \frac{2(2s-1)}{s} - \frac{2s-1}{s^2}\psi\left(\frac{1}{2s}\right)\\
&= 4\sqrt{2} - 4 - \frac{2(2s-1)}{s} + \frac{2s-1}{s^2}\left(\gamma + 2s + Z\left(\frac{1}{2s}\right)\right)\\
&= 4\sqrt{2} - 4 + \frac{2s-1}{s^2}\left(\gamma + Z\left(\frac{1}{2s}\right)\right)\\
&\geqslant 4\sqrt{2} - 4 - \frac{2s-1}{s^2}(2-\gamma)\\
&\geqslant 4\sqrt{2} - 4 - 2 + \gamma,
\end{aligned}$$

which is strictly positive.

This observation and (40) entail that $\mathcal{E}_1$ is strictly convex for large T, and consequently, the minimum in (39) is attained at a unique point that we denote by s_T. Since

$$\lim_{T\to\infty} \overline{s}_T = \frac{1}{2},$$

we thus obtain from (39) that

$$\lim_{T\to\infty} s_T = \frac{1}{2},$$

which concludes the analytical proof of (17).

A.2 Analytical verification of (19)

We point out that

$$\lim_{s\searrow 1/2} \mathcal{E}_2(s;T) = +\infty, \tag{41}$$

since the denominator in the definition of $\mathcal{E}_2$ in (15) vanishes. Moreover, since the Riemann Zeta Function vanishes at the negative even integers (different from -1), we note that $\zeta(-2)=0$, whence

$$\lim_{s\nearrow 1} \mathcal{E}_2(s;T) = 0. \tag{42}$$

Also, in light of (15), we can rewrite $\mathcal{E}_2(s;T)$ as

$$\mathcal{E}_2(s;T) = 2\pi (h(s))^{\frac{1}{2s}} \mathcal{E}_1(s,T),$$

where we have defined $h(s) := -2\zeta(-2s) > 0$ for each $s \in (1/2,1)$.

We remark[5] that, if $s\in(1/2,1)$,

$$h(s) = 2^{1-2s}\pi^{-2s-1}\,\sin(\pi s)\,\Gamma(1+2s)\,\zeta(1+2s) \in \left(0, \frac{\Gamma(3)\,\zeta(2)}{\pi^2}\right] = \left(0,\frac{1}{3}\right]$$

and therefore

$$\ln(h(s)) \leqslant \ln\frac{1}{3} < 0. \tag{43}$$

Also,

$$\begin{aligned} h'(s) \;=\; & 2^{1-2s}\pi^{-2s-1}\Gamma(1+2s)\Big[2\sin(\pi s)\zeta'(1+2s) \\ & + \zeta(1+2s)\Big(\pi\cos(\pi s) + 2\sin(\pi s)\big(\psi(1+2s) - \ln 2 - \ln\pi\big)\Big)\Big]. \end{aligned} \tag{44}$$

We recall that

$$\psi(1+2s) - \ln 2 - \ln\pi \leqslant \psi(3) - \ln 2 - \ln\pi = -0.9150927...$$

and therefore we infer from (44) that

$$\begin{aligned} h'(s) \;&\leqslant\; 2^{1-2s}\pi^{-2s-1}\Gamma(1+2s)\Big[2\sin(\pi s)\zeta'(1+2s) + \pi\zeta(1+2s)\cos(\pi s)\Big] \\ &\leqslant\; 2^{1-2s}\pi^{-2s}\Gamma(1+2s)\zeta(1+2s)\cos(\pi s). \end{aligned}$$

Since the latter term is nonpositive for $s\in\left[\frac{1}{2},1\right]$, and actually strictly negative when $s\in\left(\frac{1}{2},1\right]$, the observations above yield that $h'<0$ in $\left(\frac{1}{2},1\right)$ and more precisely, for all $s\in\left(\frac{1}{2},1\right)$,

$$-C_1 < h'(s) < -C_2, \tag{45}$$

[5]Here we are using the Riemann's Functional Equation

$$\zeta(z) = 2^z\pi^{z-1}\sin\left(\frac{\pi z}{2}\right)\Gamma(1-z)\zeta(1-z).$$

where C_1 and C_2 are positive constants.

We now compute the derivative with respect to s of $\mathcal{E}_2(s;T)$ and get

$$\frac{d}{ds}\mathcal{E}_2(s;T) = 2\pi\left[\frac{d}{ds}\mathcal{E}_1(s,T)(h(s))^{\frac{1}{2s}} + \mathcal{E}_1(s,T)(h(s))^{\frac{1}{2s}}\left(-\frac{1}{2s^2}\ln(h(s)) + \frac{1}{2s}\frac{h'(s)}{h(s)}\right)\right].$$

Hence, from equations (29) and (33) we deduce that

$$\frac{d}{ds}\mathcal{E}_2(s;T) = 2\pi c(s;T)(h(s))^{\frac{1-2s}{2s}}\Big(P(s,T)\,h(s) - (2s-1)\,\ln(h(s))\,h(s) + s(2s-1)\,h'(s)\Big), \tag{46}$$

where

$$P(s,T) := (2s-1)\ln T + (2s-1)\gamma - 2s + (2s-1)\,Z\left(\frac{1}{2s}\right)$$

and c and Z are as defined in (27) and (31), respectively.

Now, using (34) and (35), we observe that

$$\begin{aligned} P(s,T) &= (2s-1)\ln T + (2s-1)\gamma - 2s + (2s-1)\,Z\left(\frac{1}{2s}\right) \\ &= (2s-1)\ln T + (2s-1)\gamma - 2s - 2(2s-1) + (2s-1)\left(2 + Z\left(\frac{1}{2s}\right)\right) \\ &\geqslant (2s-1)\ln T + (2s-1)\gamma - 2s - 2(2s-1) \\ &= \frac{f(s)}{c(s;T)}. \end{aligned}$$

As a consequence, owing also to (43), (45) and (46) we find that

$$\begin{aligned} \frac{d}{ds}\mathcal{E}_2(s;T) &\geqslant 2\pi c(s;T)\,(h(s))^{\frac{1-2s}{2s}}\left(\frac{f(s)\,h(s)}{c(s;T)} + s(2s-1)\,h'(s)\right) \\ &\geqslant 2\pi c(s;T)\,(h(s))^{\frac{1-2s}{2s}}\left(\frac{f(s)\,h(s)}{c(s;T)} - s(2s-1)C_1\right). \end{aligned} \tag{47}$$

Consequently, by (38) and the fact that $h(s)$ is decreasing, we get that for all $s \in \big(\overline{s}_T, \frac{3}{4}\big)$,

$$2\pi c(s;T)h(s)^{\frac{1-2s}{2s}}\left(\frac{f(s)\,h(3/4)}{c(s;T)} - s(2s-1)C_1\right) \leqslant \frac{d}{ds}\mathcal{E}_2(s;T) \tag{48}$$

where $\overline{s}_T$ is as defined in (37). Now we set

$$\hat{s}_T := \overline{s}_T + \frac{1}{2}\left(\frac{s(2s-1)C_1}{h(3/4)\big(\ln T - 3 + \gamma\big)}\right) = \frac{1}{2}\left(\frac{\ln T - 2 + \gamma + s(2s-1)C_1/h(3/4)}{\ln T - 3 + \gamma}\right).$$

Hence, recalling again (35) and assuming T conveniently large, for all $s \in \big(\hat{s}_T, \frac{3}{4}\big)$,

$$\begin{aligned} \frac{f(s)h(3/4)}{c(s;T)} - s(2s-1)C_1 &= h(3/4)\Big((2s-1)\ln T + (2s-1)\gamma - 2s - 2(2s-1)\Big) - s(2s-1)C_1 \\ &= 2s\,h(3/4)\Big(\ln T + \gamma - 3\Big) + h(3/4)\Big(-\ln T - \gamma + 2\Big) - s(2s-1)C_1 \\ &> 2\hat{s}_T\,h(3/4)\Big(\ln T + \gamma - 3\Big) + h(3/4)\Big(-\ln T - \gamma + 2\Big) - s(2s-1)C_1 \\ &= 0. \end{aligned}$$

Plugging this information into (48) we find that, for large T, the function $\left(\frac{1}{2},1\right) \ni s \mapsto \mathcal{E}_2(s;T)$ is strictly increasing in $\left(\hat{s}_T,\frac{3}{4}\right)$ and in view of (41) we obtain that this function possesses a local minimum $s_T \in \left(\frac{1}{2},\hat{s}_T\right]$ and (recalling also (42)) a local maximum $S_T \in \left[\frac{3}{4},1\right)$. Since $\hat{s}_T$ converges to $\frac{1}{2}$ as $T \to +\infty$, we also obtain that $s_T \to \frac{1}{2}$ as $T \to +\infty$.

Accordingly, to complete the proof of (19), it only remains to check that $S_T \to 1$ as $T \to +\infty$. To this end, we note that, by (35) and (47),

$$\begin{aligned} 0 &= \frac{1}{2\pi c(S_T;T)\,h(S_T)^{\frac{1-2S_T}{2S_T}}}\,\frac{d}{ds}\mathcal{E}_2(S_T;T) \geqslant \frac{f(S_T)\,h(S_T)}{c(S_T;T)} - S_T(2S_T-1)C_1 \\ &= h(S_T)\Big((2S_T-1)\ln T + (2S_T-1)\gamma - 2S_T - 2(2S_T-1)\Big) - S_T(2S_T-1)C_1 \\ &\geqslant h(S_T)\frac{\ln T}{2} - C_2 - C_3 h(S_T), \end{aligned}$$

for some constants C_2, $C_3 > 0$.

For this reason,

$$\lim_{T\to+\infty} \frac{C_2}{h(S_T)} + C_3 \geqslant \lim_{T\to+\infty} \frac{\ln T}{2} = +\infty,$$

whence

$$0 = \lim_{T\to+\infty} h(S_T) = \lim_{T\to+\infty} -2\zeta(-2s_T).$$

Since the only zero of the Riemann Zeta Function in $[-2,-1]$ occurs at -2, we thereby infer that $-2s_T \to -2$, and thus $s_T \to 1$, as $T \to +\infty$. With this, we have concluded the analytical verification of (19).

A.3 Analytical verification of (24)

We observe that

$$\begin{aligned} &\mathcal{P}(s;L,T) \\ :=\;& \frac{4\pi\,L^{1+2s}\,\zeta(2s)}{T\Gamma(1+2s)}\,\frac{d}{ds}\mathcal{G}_3(s;L,T) \\ =\;& \zeta(1+2s)\Big(-2\ln L\,\sin(\pi s) + \pi\cos(\pi s) + 2\sin(\pi s)\psi(1+2s)\Big) + 2\sin(\pi s)\zeta'(1+2s) \\ & -\frac{2\zeta(1+2s)\sin(\pi s)\zeta'(2s)}{\zeta(2s)} \end{aligned}$$

and the positivity of the derivative of $\mathcal{G}_3$ is equivalent to the positivity of $\mathcal{P}$.

We also recall that near $z = 1$ the derivative of the Riemann Zeta Function has the Laurent expansion

$$\frac{\zeta'(z)}{\zeta(z)} = -\frac{1}{z-1} + \gamma + O(z-1), \tag{49}$$

see e.g. page 481 in [14].

Let also

$$\mathcal{Q}(s) := \zeta(1+2s)\Big(\pi\cos(\pi s) + 2\sin(\pi s)\psi(1+2s)\Big) + 2\sin(\pi s)\zeta'(1+2s)$$

and note that $\sup_{s\in\left(\frac{1}{2},1\right)} |\mathcal{Q}(s)| \leqslant C$ for some $C > 0$; in addition,

$$\mathcal{P}(s;L,T) \;=\; -2\zeta(1+2s)\ln L\,\sin(\pi s) - \frac{2\zeta(1+2s)\sin(\pi s)\zeta'(2s)}{\zeta(2s)} + \mathcal{Q}(s)$$

$$
\begin{aligned}
&= -2\zeta(1+2s)\sin(\pi s)\left(\ln L + \frac{\zeta'(2s)}{\zeta(2s)}\right) + \mathcal{Q}(s)\\
&= -2\zeta(1+2s)\sin(\pi s)\left(\ln L - \frac{1}{2s-1}\right) + \widetilde{\mathcal{Q}}(s),
\end{aligned}
$$

where

$$
\widetilde{\mathcal{Q}}(s) := \mathcal{Q}(s) - 2\zeta(1+2s)\sin(\pi s)\left(\frac{\zeta'(2s)}{\zeta(2s)} + \frac{1}{2s-1}\right).
$$

We stress that $\sup_{s\in\left(\frac{1}{2},1\right)} |\widetilde{\mathcal{Q}}(s)| \leqslant \widetilde{C}$ for some $\widetilde{C} > 0$, thanks to (49).

Let now

$$
\varepsilon_L := \frac{1}{\sqrt{\ln L}} \qquad \text{and} \qquad s_L^{(\pm)} := \frac{1}{2} + \frac{1 \pm \varepsilon_L}{2\ln L}.
$$

We notice that

$$
\lim_{L\to+\infty} \varepsilon_L = 0 \qquad \text{and} \qquad \lim_{L\to+\infty} s_L^{(\pm)} = \frac{1}{2}. \tag{50}
$$

Also, when $s \in \left(\frac{1}{2}, s_L^{(-)}\right]$, we have that

$$
2s - 1 \leqslant 2s_L^{(-)} - 1 = \frac{1-\varepsilon_L}{\ln L}
$$

and, as a result, for large L,

$$
\begin{aligned}
\mathcal{P}(s;L,T) &\geqslant 2\zeta(1+2s)\sin(\pi s)\left(-\ln L + \frac{\ln L}{1-\varepsilon_L}\right) - \widetilde{C}\\
&= \frac{2\varepsilon_L \ln L\, \zeta(1+2s)\sin(\pi s)}{1-\varepsilon_L} - \widetilde{C}\\
&\geqslant \sqrt{\ln L}\, \zeta(1+2s)\sin(\pi s) - \widetilde{C}\\
&\geqslant \frac{\sqrt{\ln L}\, \zeta(3)}{2} - \widetilde{C}\\
&> 0.
\end{aligned}
$$

Instead, when $s \in \left[s_L^{(+)}, 1\right)$,

$$
2s - 1 \geqslant 2s_L^{(+)} - 1 = \frac{1+\varepsilon_L}{\ln L},
$$

which entails that

$$
\begin{aligned}
\mathcal{P}(s;L,T) &\leqslant 2\zeta(1+2s)\sin(\pi s)\left(-\ln L + \frac{\ln L}{1+\varepsilon_L}\right) + \widetilde{\mathcal{Q}}(s)\\
&\leqslant -\frac{2\varepsilon_L \ln L\, \zeta(1+2s)\sin(\pi s)}{1+\varepsilon_L} + \mathcal{Q}(s) + C_1\sin(\pi s)\\
&\leqslant -\frac{2\sqrt{\ln L}\, \zeta(3)\sin(\pi s)}{1+\varepsilon_L} + \pi\cos(\pi s)\zeta(1+2s) + C_2\sin(\pi s)\\
&= -\sin(\pi s)\left(\frac{2\sqrt{\ln L}\, \zeta(3)}{1+\varepsilon_L} - C_2\right) + \pi\cos(\pi s)\zeta(1+2s)\\
&\leqslant -\sin(\pi s)\left(\sqrt{\ln L}\, \zeta(3) - C_2\right) + \pi\cos(\pi s)\zeta(1+2s)
\end{aligned}
$$

$$< \ 0,$$

where C_1 and C_2 are suitable positive constants.

From these considerations, it follows that there exists at least one zero for $\mathcal{P}$ and all the zeros of $\mathcal{P}$ are located in $\left(s_L^{(-)}, s_L^{(+)}\right)$. As a consequence,

$$\begin{aligned} &\text{there exists at least a critical point for } \mathcal{G}_3 \\ &\text{and all the critical points of } \mathcal{G}_3 \text{ are located in } \left(s_L^{(-)}, s_L^{(+)}\right). \end{aligned} \tag{51}$$

We now show that

$$\mathcal{P} \text{ is strictly decreasing in } \left(s_L^{(-)}, s_L^{(+)}\right). \tag{52}$$

For this, we calculate that

$$\begin{aligned} \frac{d}{ds}\mathcal{P}(s;L,T) \ &= \ \ln L\Big(-4\sin(\pi s)\zeta'(1+2s) - 2\pi\zeta(1+2s)\cos(\pi s)\Big) \\ &\quad + \pi\cos(\pi s)\left[4\zeta'(1+2s) + 2\zeta(1+2s)\left(\psi(1+2s) - \frac{\zeta'(2s)}{\zeta(2s)}\right)\right] \\ &\quad + 4\sin(\pi s)\left[\zeta''(1+2s) + \zeta'(1+2s)\left(\psi(1+2s) - \frac{\zeta'(2s)}{\zeta(2s)}\right)\right. \\ &\qquad \left. + \zeta(1+2s)\left(-\frac{\zeta''(2s)}{\zeta(2s)} + \left(\frac{\zeta'(2s)}{\zeta(2s)}\right)^2 + \psi'(1+2s) - \pi^2\right)\right] \\ &\leqslant \ \ln L\Big(-4\sin(\pi s)\zeta'(1+2s) - 2\pi\zeta(1+2s)\cos(\pi s)\Big) \\ &\quad - \pi\cos(\pi s)\frac{\zeta'(2s)}{\zeta(2s)} - 4\sin(\pi s)\frac{\zeta'(2s)}{\zeta(2s)} \\ &\quad + \zeta(1+2s)\left(-\frac{\zeta''(2s)}{\zeta(2s)} + \left(\frac{\zeta'(2s)}{\zeta(2s)}\right)^2\right) + C_3 \end{aligned} \tag{53}$$

for some constant $C_3 > 0$.

Additionally, differentiating the Laurent expansion in (49),

$$\frac{\zeta''(z)}{\zeta(z)} - \left(\frac{\zeta'(z)}{\zeta(z)}\right)^2 = \frac{d}{dz}\frac{\zeta'(z)}{\zeta(z)} = \frac{1}{(z-1)^2} + O(1).$$

Plugging this information into (53) we find that

$$\begin{aligned} \frac{d}{ds}\mathcal{P}(s;L,T) \ &\leqslant \ \ln L\Big(-4\sin(\pi s)\zeta'(1+2s) - 2\pi\zeta(1+2s)\cos(\pi s)\Big) \\ &\quad - \pi\cos(\pi s)\frac{\zeta'(2s)}{\zeta(2s)} - 4\sin(\pi s)\frac{\zeta'(2s)}{\zeta(2s)} - \frac{\zeta(1+2s)}{(2s-1)^2} + C_4 \end{aligned}$$

for some constant $C_4 > 0$. Thus, since $\zeta' \leqslant 0$,

$$\begin{aligned} \frac{d}{ds}\mathcal{P}(s;L,T) \ &\leqslant \ \ln L\Big(-4\sin(\pi s)\zeta'(1+2s) - 2\pi\zeta(1+2s)\cos(\pi s)\Big) \\ &\quad - \frac{4\zeta'(2s)}{\zeta(2s)} - \frac{\zeta(1+2s)}{(2s-1)^2} + C_4 \\ &\leqslant \ \ln L\Big(-4\sin(\pi s)\zeta'(1+2s) - 2\pi\zeta(1+2s)\cos(\pi s)\Big) \\ &\quad + \frac{4}{2s-1} - \frac{\zeta(1+2s)}{(2s-1)^2} + C_5 \end{aligned} \tag{54}$$

for some $C_5 > 0$, where (49) has been used once again.

Moreover, if $s \in \left(\frac{1}{2}, s_L^{(+)}\right]$, then, for large L,

$$2s - 1 \leqslant \frac{1+\varepsilon_L}{\ln L} \leqslant \frac{2}{\ln L}$$

and therefore we deduce from (54) that

$$\begin{aligned}\frac{d}{ds}\mathcal{P}(s;L,T) &\leqslant \frac{C_6}{2s-1} - \frac{\zeta(1+2s)}{(2s-1)^2} \leqslant \frac{1}{2s-1}\left(C_6 - \frac{\zeta(3)}{2s-1}\right) \\ &\leqslant -\frac{1}{2s-1}\left(\frac{\zeta(3)}{2s_L^{(+)}-1} - C_6\right) \leqslant -\frac{1}{2s-1}\left(\frac{\zeta(3)\,\ln L}{2} - C_6\right) < 0,\end{aligned}$$

which completes the proof of (52).

The desired claim in (24) now follows combining (51) and (52) with the second limit in (50).

A.4 Analytical verification of (26)

We start by computing the derivative of $\mathcal{G}_4$ with respect to s, and we get that

$$\frac{d}{ds}\mathcal{G}_4(s,T,L) = -\frac{T}{4L^{1+2s}\,\zeta(2s)}\left(\ln L + \frac{\zeta'(2s)}{\zeta(2s)}\right). \tag{55}$$

Now we observe that, for $s \in \left(\frac{1}{2}, 1\right)$, the function

$$m(s) := \frac{\zeta'(2s)}{\zeta(2s)}$$

is negative and strictly increasing. Furthermore, from (49) we infer that

$$\lim_{s \searrow 1/2} m(s) = -\infty. \tag{56}$$

Now, in light of (55),

$$\begin{aligned}&\frac{d}{ds}\mathcal{G}_4(s,T,L) > 0 \text{ if and only if } \ln L + m(s) < 0, \\ &\text{and thus if and only if } L < \exp\left(-m(s)\right).\end{aligned} \tag{57}$$

Also, from (25) and the monotonicity of the function m, for each $L \leqslant L^\star$ and $s \in \left(\frac{1}{2}, 1\right)$ we have that

$$\exp\left(-m(s)\right) > \exp\left(-m(1)\right) = L^\star \geqslant L,$$

and therefore we deduce from (57) that

$$\text{when } L \leqslant L^\star \text{ the supremum of } \left(\tfrac{1}{2}, 1\right) \ni s \mapsto \mathcal{G}_4(s;L,T) \text{ is uniquely attained at } s = 1. \tag{58}$$

If instead $L > L^\star$, using (56) we see that

$$\lim_{s \searrow 1/2} \exp\left(-m(s)\right) = +\infty > L$$

$$\text{and} \qquad \lim_{s\nearrow 1} \exp\left(-m(s)\right) = \exp\left(-m(1)\right) = L^\star < L.$$

This and the strict monotonicity of m yield that for each $L > L^\star$ there exists a unique $s_L \in \left(\frac{1}{2}, 1\right)$ such that

$$\frac{d}{ds}\mathcal{G}_4(s_L, L, T) = 0, \tag{59}$$

with $\frac{d}{ds}\mathcal{G}_4(s, L, T) > 0$ if and only if $s \in \left(\frac{1}{2}, s_L\right)$, namely s_L is the unique maximum for $\mathcal{G}_4(s, L, T)$ when $L > L^\star$.

From these observations and (58), in order to complete the analytical proof of (26), it is only left to show that

$$\lim_{L\to+\infty} s_L = \frac{1}{2}. \tag{60}$$

To this end, equations (55) and (59) give that

$$0 = \ln L + m(s_L),$$

which leads to

$$+\infty = \lim_{L\to+\infty} \ln L = -\lim_{L\to+\infty} m(s_L). \tag{61}$$

Since the only pole of $m(s)$ at $\left[\frac{1}{2}, 1\right]$ occurs in $s = \frac{1}{2}$, then we obtain (60), as desired.

References

[1] N. Abatangelo, E. Valdinoci, *Getting acquainted with the fractional Laplacian*. Contemporary research in elliptic PDEs and related topics, 1–105, Springer INdAM Ser., 33, Springer, Cham, 2019.

[2] J. Bonnar, *The Gamma Function*. Treasure Trove of Mathematics, Danvers, MA, 2017. vii+149 pp.

[3] V. V. Afanasiev, R. Z. Sagdeev, G. M. Zaslavsky, *Chaotic jets with multifractal space-time random walk*. Chaos 1 (1991), 143–159.

[4] R. P. D. Atkinson, C. J. Rhodes, D. W. Macdonald, R. M. Anderson, *Scale-free dynamics in the movement patterns of jackals*. Oikos 98 (2002), 134–140.

[5] F. Bartumeus, J. Catalan, U. L. Fulco, M. L. Lyra, G. M. Viswanathan, *Optimizing the encounter rate in biological interactions: Lévy versus Brownian strategies*. Phys, Rev. Lett. 88 (2002), 097901:1–4.

[6] F. Bartumeus, M. G. E. da Luz, G. M. Viswanathan, J. Catalan, *Animal search strategies: a quantitative random-walk analysis*. Ecology, 86 (2005), 3078–3087.

[7] S. Benhamou, *How many animals really do the Lévy walk?* Ecology 88 (2007), 1962–1969.

[8] S. Bertrand, J. M. Burgos, F. Gerlotto, J. Atiquipa, *Lévy trajectories of Peruvian purse-seiners as an indicator of the spatial distribution of anchovy*. ICES J. Marine Sci. 62 (2005), 477–482.

[9] D. Boyer, G. Ramos-Fernández, O. Miramontes, J. L. Mateos, G. Cocho, H. Larralde, H. Ramos, F. Rojas, *Scale-free foraging by primates emerges from their interaction with a complex environment*. Proc. R. Soc. B. 273 (2006), 1743–1750.

[10] D. Brockmann, L. Hufnagel, T. Geisel, *The scaling laws of human travel*. Nature 439 (2006), 462–465.

[11] C. T. Brown, L. S. Liebovitch, R. Glendon, *Lévy Flights in Dobe Ju/'hoansi Foraging Patterns*. Hum. Ecol. 35 (2007), 129–138.

[12] S. V. Buldyrev, S. Havlin, A. Y. Kazakov, M. G. da Luz, E. P. Raposo, H. E. Stanley, G. M. Viswanathan, *Average time spent by Lévy flights and walks on an interval with absorbing boundaries*. Phys. Rev. E 64 (2001), 041108:1–11.

[13] S. V. Buldyrev, E. P. Raposo, F. Bartumeus, S. Havlin, F. R. Rusch, M. G. E. da Luz, G. M. Viswanathan, *Comment on "Inverse Square Lévy Walks are not Optimal Search Strategies for d⩾2"*. Phys. Rev. Lett. 126 (2021), 048901:1–2.

[14] B. K. Choudhury, *The Riemann zeta-function and its derivatives*. Proc. Roy. Soc. London Ser. A 450 (1995), 477–499.

[15] G. M. Coclite, S. Dipierro, G. Fanizza, F. Maddalena, E. Valdinoci, *Dispersive effects in a peridynamic model*. Preprint `https://arxiv.org/abs/2105.01558` (2021)

[16] A. M. Edwards, R. A. Phillips, N. W. Watkins, M. P. Freeman, E. J. Murphy, V. Afanasyev, S. V. Buldyrev, M. G. E. da Luz, E. P. Raposo, H. E. Stanley, G. M. Viswanathan, *Revisiting Lévy flight search patterns of wandering albatrosses, bumblebees and deer*. Nature 449 (2007), 1044–1048.

[17] K. Garg, C. T. Kello, *Efficient Lévy walks in virtual human foraging*. Scient. Rep. 11 (2021), 5242:1–12.

[18] A. O. Gautestad, A. Mysterud, *The Lévy flight foraging hypothesis: forgetting about memory may lead to false verification of Brownian motion*. Movement Ecol. 1 (2013), 1–9.

[19] I. M. Gel'fand, G. E. Shilov, *Generalized functions*. Volume 1. Properties and operations. Academic Press, New York-London, 1964. xviii+423 pp.

[20] M. C. González, C. A. Hidalgo, A.-L. Barabási, *Understanding individual human mobility patterns*, Nature 453 (2008), 779–782.

[21] R. D. Gray, *Faith and foraging: a critique of the "paradigm argument from design"*. Foraging Behavior. Springer, Boston, 1987. x+676 pp. ISBN: 978-1-4613-1839-2.

[22] G. C. Hays, T. Bastian, T. K. Doyle, S. Fossette, A. C. Gleiss, M. B. Gravenor, V. J. Hobson, N. E. Humphries, M. K. S. Lilley, N. G. Pade, D. W. Sims, *High activity and Lévy searches: jellyfish can search the water column like fish*. Proc. R. Soc. B 279 (2012), 465–473.

[23] N. E. Humphries, N. Queiroz, J. R. M. Dyer, N. G. Pade, M. K. Musyl, K. M. Schaefer, D. W. Fuller, J. M. Brunnschweiler, T. K. Doyle, J. D. R. Houghton, G. C. Hays, C. S. Jones, L. R. Noble, V. J. Wearmouth, E. J. Southall, D. W. Sims, *Environmental context explains Lévy and Brownian movement patterns of marine predators*. Nature 465 (2010), 1066–1069.

[24] N. E. Humphries, H. Weimerskirch, N. Queiroz, E. J. Southall, D. W. Sims, *Foraging success of biological Lévy flights recorded in situ*. Proc. Nat. Acad. Sci. U.S.A. 109 (2012), 7169–7174.

[25] N. E. Humphries, H. Weimerskirch, D. W. Sims, *A new approach for objective identification of turns and steps in organism movement data relevant to random walk modelling*. Meth. Ecol. Evol. 4 (2013), 930–938.

[26] A. James, M.J. Plank, A. M. Edwards, *Assessing Lévy walks as models of animal foraging*. J. R. Soc. Interface 8 (2011), 1233–1247.

[27] N. Levernier, J. Textor, O. Bénichou, R. Voituriez, *Inverse Square Lévy Walks are not Optimal Search Strategies for d⩾2*. Phys. Rev. Lett. 124 (2020), 080601:1–5.

[28] N. Levernier, J. Textor, O. Bénichou, R. Voituriez, *Reply to "Comment on 'Inverse Square Lévy Walks are not Optimal Search Strategies for d⩾2"'*. Phys. Rev. Lett. 126 (2021),048902:1.

[29] A. Mårell, J. P. Ball, A. Hofgaard, *Foraging and movement paths of female reindeer: insights from fractal analysis, correlated random walks, and Lévy flights*. Can. J. Zool. 80 (2002), 854–865.

[30] E. W. Montroll, G. H. Weiss, *Random walks on lattices. II*. J. Mathematical Phys. 6 (1965), 167–181.

[31] V. V. Palyulin, A. V. Chechkin, R. Metzler, *Lévy flights do not always optimize random blind search for sparse targets*. Proc. Nat. Acad. Sci. U.S.A. 111 (2014), 2931–2936.

[32] G. J. Pierce, J. G. Ollason, *Eight reasons why optimal foraging theory is a complete waste of time*, Oikos 49 (1987), 111–118.

[33] M. A. Pinsky, *Introduction to Fourier analysis and wavelets*. Brooks/Cole Series in Advanced Mathematics. Brooks/Cole, Pacific Grove, CA, 2002. xviii+376 pp. ISBN: 0-534-37660-6.

[34] G. Pólya, *On the zeros of an integral function represented by Fourier's integral*. Messenger of Math. 52 (1923), 185–188.

[35] H. Rademacher, *Topics in analytic number theory*. Die Grundlehren der mathematischen Wissenschaften, Band 169. Springer-Verlag, New York-Heidelberg, 1973. ix+320 pp.

[36] D. A. Raichlen, B. M. Wood, A. D. Gordon, A. Z. P. Mabulla, F. W. Marlowe, H. Pontzer, *Evidence of Lévy walk foraging patterns in human hunter-gatherers*. Proc. Nat. Acad. Sci. U.S.A. 111 (2014), 728–733.

[37] E. P. Raposo, S. V. Buldyrev, M. G. E. da Luz, G. M. Viswanathan, H. E. Stanley, *Lévy flights and random searches*. J. Phys. A 42 (2009), 434003:1–23.

[38] A. M. Reynolds, *Mussels realize Weierstrassian Lévy walks as composite correlated random walks*. Sci. Rep. 4 (2014), 4409:1–5.

[39] A. Reynolds, E. Ceccon, C. Baldauf, T. K. Medeiros, O. Miramontes, *Lévy foraging patterns of rural humans*. PLoS ONE 13 (2018), e0199099:1–16.

[40] A. M. Reynolds, M. A. Frye, *Free-Flight Odor Tracking in Drosophila Is Consistent with an Optimal Intermittent Scale-Free Search*. PLoS ONE 2 (2007), e354:1–9.

[41] A. M. Reynolds, N. T. Ouellette, *Swarm dynamics may give rise to Lévy flights*. Sci. Rep. 6 (2016), 30515:1–8.

[42] A. M. Reynolds, A. D. Smith, R. Menzel, U. Greggers, D. R. Reynolds, J. R. Riley, *Displaced honey bees perform optimal scale-free search flights*. Ecology 88 (2007), 1955–1961.

[43] M. F. Shlesinger, J. Klafter, Y. M. Wong, *Random walks with infinite spatial and temporal moments*. J. Statist. Phys. 27 (1982), 499–512.

[44] M. F. Shlesinger, B. J. West, J. Klafter, *Lévy Dynamics of Enhanced Diffusion: Application to Turbulence*. Phys. Rev. Lett. 58 (1987), 1100-1103.

[45] M. F. Shlesinger, G. M. Zaslavsky, J. Klafter, *Strange kinetics*. Nature 363 (1993), 31–37.

[46] D. W. Sims, E. J. Southall, N. E. Humphries, G. C. Hays, C. J. A. Bradshaw, J. W. Pitchford, A. James, M. Z. Ahmed, A. S. Brierley, M. A. Hindell, D. Morritt, M. K. Musyl, D. Righton, E. L. C. Shepard, V. J.Wearmouth, R. P. Wilson, M. J. Witt, J. D. Metcalfe, *Scaling laws of marine predator search behaviour*. Nature 451 (2008), 1098–1102.

[47] D. W. Stephens, J. R. Krebs, *Foraging Theory*. Monographs in Behavior and Ecology. Princeton University Press, Princeton, NJ, 1986. xiv+247 pp. ISBN: 9780691084428.

[48] V. Vallaeys, R. C. Tyson, W. D. Lane, E. Deleersnijder, E. Hanert, *A Lévy flight diffusion model to predict transgenic pollen dispersal*. J. R. Soc. Interface 14 (2017), 20160889:1–10.

[49] G. M. Viswanathan, V. Afanasyev, S. V. Buldyrev, S. Havlin, S., M. G. da Luz, E. Raposo, H. E. Stanley, *Lévy flights in random searches*. Phys. A 282 (2000), 1–12.

[50] G. M. Viswanathan, F. Bartumeus, S. V. Buldyrev, J. Catalan, U. L. Fulco, S. Havlin, M. G. E. da Luz, M. L. Lyra, E. P. Raposo, H. E. Stanley, *Lévy flight random searches in biological phenomena*. Horizons in complex systems (Messina, 2001). Phys. A 314 (2002), 208–213.

[51] G. M. Viswanathan, S. V. Buldyrev, S. Havlin, M. G. da Luz, E. P. Raposo, H. E. Stanley, *Optimizing the success of random searches*. Nature 401 (1999), 911-914.